2018

An Autothermal, Representative Scale Test Of Compost Heat Potential Using Geostatistical Analysis

William J. McCune-Sanders
University of Vermont

AN AUTOTHERMAL, REPRESENTATIVE SCALE TEST OF COMPOST HEAT POTENTIAL USING GEOSTATISTICAL ANALYSIS

A Thesis Presented

by

W. Jason McCune-Sanders

to

The Faculty of the Graduate College

of

The University of Vermont

In Partial Fulfillment of the Requirements
for the Degree of Master of Science
Specializing in Mechanical Engineering

January, 2018

Defense Date: November 10, 2017
Thesis Examination Committee:

Darren L. Hitt, Ph.D., Advisor
Donna M. Rizzo, Ph.D., Chairperson
William F. Louisos, Ph.D.
Cynthia J. Forehand, Ph.D., Dean of the Graduate College

ABSTRACT

Composting has been practiced for thousands of years as a way of stabilizing and recycling organic matter into useful soil amendments. Thermophilic compost releases significant amounts of heat at temperatures (~140 °F) that are useful for environmental heating or process water. This heat has been taken advantage of in various ways throughout history, but development of a widely adopted technology remains elusive.

The biggest barrier to adoption of compost heat recovery (CHR) systems is projecting accurate, attractive economic returns. The cost of transfer equipment is significant, and with variability in composting substrates and methods, it is difficult to predict the power and quality of heat a proposed system would produce. While the ultimate heat release may be calculated with standard techniques, the dynamics of compost temperature and thermal power are less understood. As heat yield is one of many goals, better understanding of compost's thermal dynamics is important for CHR optimization. This research addresses the issue by developing a field test that measures heat release and temperature across a representative-scale compost volume.

The compost test vessel was built from common construction materials and insulated enough to be self-heating in cold weather. A 4' x 4' x 4' cube of 2" foam insulation panels held 1.812 cubic yards of active compost, intermittently aerated at ~35 CFM. Data from 84 temperature sensors, and one pressure sensor at the blower, was logged at 1-minute intervals for a period of 35 days. Spatial temperature fields were estimated by Kriging, and used to calculate conductive heat loss and compost volume temperature over time. Enthalpy loss was calculated using the blower pressure curve, temperature data and humidity assumptions.

The compost exhibited wide variation in temperature and heat flow over time, and less horizontal symmetry than expected. The results are dynamic and best viewed graphically. Enthalpy loss varied with adjustments to the aeration cycle, ranging from 100 to 550 W (60-minute average rates), while conductive losses were in the range of 75 W. Peak sustained thermal output was around 600 W (500 W by aeration) from days 11-13 with about 0.6 yd^3 of compost in the thermophilic zone; however, this cooled the compost significantly. Aeration was then reduced, and the compost temperature recovered, with 50% - 90% of the compost volume above 130 °F from days 14-23; during this period, total heat loss was around 150 - 200 W with aeration loss around 60-100 W.

The test was successful in producing hot compost and building temperature field and heat loss models. However representative aeration rates cooled a large amount of the compost volume as cool air was drawn into the vessel. Aeration rate reduction accomplished desired compost temperatures, but resulted in low enthalpy extraction rate and temperature. Future work will address this issue with the ability to recirculate air through the compost.

DEDICATIONS

This thesis is dedicated to two role models in my life who passed away this fall:

My grandfather William James McCune-Sanders, who was a mechanical engineer and, although often stern, was supportive of my various ideas and unusual career over the years and provided objective, unfiltered feedback few others would. Bill passed away this year at the old age of 102.

Jim H. Foster Jr., formerly of Vt. Natural Ag. Products, who was an enthusiastic leader in our two compost heat recovery projects at their compost operation in Middlebury, and worked alongside us to develop solutions to the design challenges along the way. Jim died in a tragic farm accident at the age of 47.

ACKNOWLEDGMENTS

My advisor, Dr. Darren Hitt, taught me the fundamentals of heat transfer, and agreed to take me on as a graduate student with an unusual, self-directed project. Darren also encouraged me to apply for the SBIR-0 grant which provided critical funding.

Dr. Donna Rizzo, committee chair, has also been an advisor and valuable ally as my work with compost heat has evolved over the past 8 years, and taught me the geostatistical techniques that are central to this thesis.

Dr. William Louisos, who is not only a committee member but an old friend, and has displayed interest and feedback on this project and many others over the years, often while hiking or riding the double chair double at Mad River Glen.

Others who have been instrumental include: Dr. Guy Roberts, my friend and former boss (or colleague as he generously put it), who pretty much forced me to become an engineer in 2004; Brian Jerose, owner of Agrilab Technologies and a leader in the compost heat field, has enabled my work; Dan Heyde who hosted this experiment; Dave Whitney who hosted my original project of this type; Karl Hammer of VT Compost Co. who provided wry humor and high quality compost feedstock.

My family: Parents Joe and Gigi who have provided support when needed throughout my late term student-ship, and my wife Ellen who puts up with all this and takes care of me when things get crazy.

The SBIR Phase-0 provided much of the necessary funding for this effort.

TABLE OF CONTENTS:

LIST OF FIGURES

CHAPTER 1: Introduction

1.1. Introduction

Composting is defined here as the accelerated decomposition of organic matter by thermophilic, aerobic bacteria. In nearly all compost system, thermophilic temperatures (above approximately 45 °C or 132 °F [1]) are achieved and maintained by the heat released from biological activity. The process occurs naturally and spontaneously in masses of organic material when conditions are right, usually shortly after accumulation of raw substrate [2].

In other words, successful compost systems (except for small-scale heated reactors) heat themselves, which requires maintaining proper conditions including substrate composition, moisture content, oxygen content, temperature, and insulation (to allow heat to accumulate). Insulation is typically achieved by increasing volume to allow the inner portions to become thermophilic, while the outside remains cool and decomposes more slowly. The thermophilic core also tends to become oxygen deprived. In small to medium systems, this is typically managed by turning the compost pile to mix it, but aeration by passive (enhanced natural convection) or active (forced convection) is also employed.

Excessive heat buildup can elevate temperatures above the ideal thermophilic limit (150 °F to 170 °F), slowing biological activity, and leading to spontaneous combustion in extreme cases. In large or highly insulated systems, active aeration or high turning frequency becomes necessary to cool the piles as well as maintain oxygen levels.

Compost processes range in complexity from simple heaps to engineered systems with specialized equipment and feedback control algorithms. In its simplest forms, composting has been practiced by humans for thousands of years [1]. Since then, is it only natural that people are interested in the heat released by compost piles, and various methods for utilizing it have been employed but none are widely adopted.

Current optimization of industrial compost processes primarily focuses on increasing throughput relative to constraints (land availability, costs of labor, fuel or equipment). Operations such as private composters, municipal composters, and livestock farmers may focus on aspects of marketing high quality product, converting large streams of organics, or simply managing their own manures or crop residues. While many compost operators would like to use the heat released, few do so as the feasibility remains speculative.

1.2. Motivation

The biggest barrier to adoption of compost heat recovery CHR systems is projecting accurate economic returns that are attractive to businesses. For prospective adopters, the first questions are typically “How much heat can I make with my compost”, “How much would the system cost”, and “What is the payback period”. While many farms and compost sites are releasing large quantities of that they could use, the expense and scope of building a CHR system, which may include aeration channels under the compost, transfer pipes, blowers and heat exchangers, and integration with heat loads, is significant.

Large compost operations are by nature thermally efficient and often have heat production potential that exceeds heat loads at the site. Smaller CHR adopters, particularly

on-farm composters, generally operate on tight budgets and have thermal demands (on the order of $10,000-$100,000/year heating costs) that exceed their CHR potential. Thus, particularly on the smaller scale there is a need to develop thermally efficient CHR systems that are cost effective and can be operated using conventional farm or compost equipment. Larger operators could also use such technology to meet their heating needs with a smaller portion of compost.

To optimize any technology, it is important to estimate its efficiency, simply put: How much could this system produce under ideal conditions, compared to its current performance? In CHR systems, this requires knowing how much heat the compost could produce if operated optimally. The ultimate release of thermal energy by compost can be calculated by comparing raw feedstock with finished compost [3], but the dynamics of compost temperature geometry and heat release over the duration of the compost cycle are not well understood. As the heat is low quality and continually released, changes in output temperature and flow can dramatically affect the amount of energy that can be used effectively.

1.3. Research Objectives

The purpose of this research is to design a low-cost experimental platform on which compost temperatures and heat outputs can be measured over time. The approach is to develop an insulated test vessel made of common construction materials that is self-heating and does not require climate-controlled space. Vessels that are large enough to be

autothermal have the added benefit of averaging out the natural variability in compost feedstock, and exhibit behavior that is closer to full-scale compost.

This goal can be described as three research objectives. The first is to build the physical platform for the experiment, operate it successfully, and collect results. Second is to develop mathematical techniques to determine the heat production and compost temperatures over time, and produce useful outputs that can be interpreted easily. Third is to assess how the experiment could be done economically in the future, primarily by leveraging the analysis methods to reduce the number of sensors needed.

1.4. Units of Measurement

Units used in this thesis are a mixture of SI and Imperial. While most engineering is done in SI units, in the U.S. the composting industry generally uses Imperial measurements including the cubic yard (yd^3), and as building supplies and tools in the U.S. currently use inches and feet, it is more accurate and replicable to describe the compost vessel as such. SI units, however, are more convenient and commonly used in thermodynamic calculations, and the Watt is more intuitive and understood by the public than the Imperial equivalents of BTU/h, etc. In general, units are preserved from their sources and converted when appropriate, and thermodynamic calculations that begin with Imperial units of length and volume are converted to SI units of mass and energy.

CHAPTER 2: Background and Literature Review

2.1. Anecdotal and historical background

Besides the microbes and small animals that regularly inhabit compost piles, the first creatures to take advantage of compost heat probably used it to incubate their eggs. Female crocodilians bury their eggs in either hole or mounds of compost, where they incubate for two to three months. Megapodiidae is a family of chicken sized birds with strong legs and feet, found in Australia the surrounding Australasian region. They are unique among birds for incubating their eggs not by sitting on them, but by burying them in warm material, usually mounds of compost which the male constructs and tends to, adding or removing material to regulate temperature. Megapode hatchlings emerge more mature than any other bird, digging their way out of the compost pile with their feet and able to forage for themselves the same day [4].

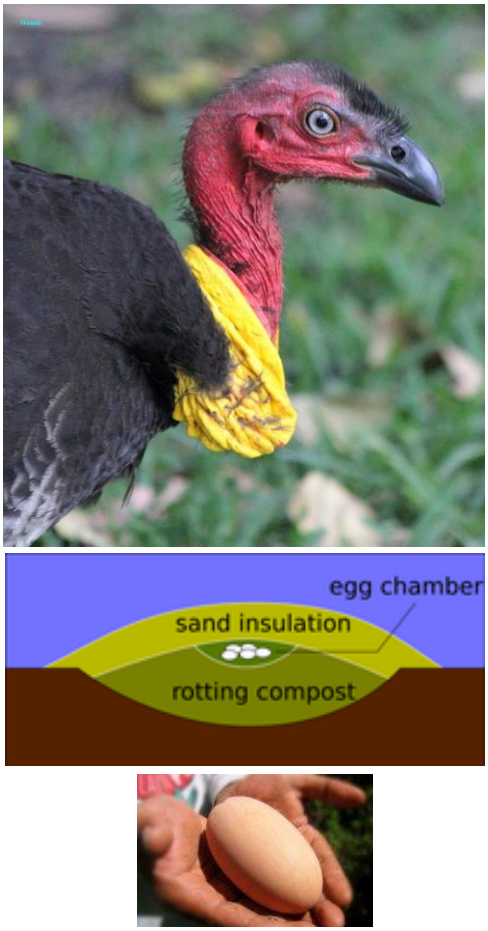

Figure 1: Australian Brush Turkey (*Megapodiidae Alectura lathami*), Incubation Mound, and Egg [4]

The earliest human uses of compost heat were to extend the growing season by planting in or near compost piles. Up to 2000 years ago, farmers in northern China used "hotbeds", trenches filled with manure and covered with soil, to extend the growing season 1 to 2 months [5]. From the

1600's to 1920's, hotbeds covered in glass were widely used by French horticulturalists for winter cropping. Their techniques were refined and optimized over the years [6], but the practice subsided as the spread of the automobile reduced the abundance of horse manure. A similar method was popular in England and Holland from around 1940 to 1970, where straw bales were soaked in manure slurry, capped with compost and planted over [7].

The first documented attempts to use compost heat indirectly, through use of a heat exchange fluid, were by the French forester Jean Pain (1928-1981), who captured heat from large (~100 yd^2) mounds of composting wood chips. Much of his work consisted of clearing underbrush and thick growth in the fire prone forests of Southern Provence, and he learned to produce high quality compost from the slash he produced, primarily by using sticks and branches <8mm diameter. In his region of poor, shallow soils and hot dry summers, the nutrient and water retaining qualities of his compost were compelling. Pain, supported by his wife and cohorts, went on to invent a tractor driven wood chipper that produced fine particles ~1mm in diameter. He constructed mounds by successively watering and compacting layers of wood chips while burying a coil of polyethylene pipe. Pain claimed his mounds would continuously heat 4 liters per minute of water from 10 to 60° C for 6 months, which is a continuous yield of nearly 14 kW, or about 140 watts per yd^3. He also placed batch digesters of wood chips within his mounds (cooled by a pipe coil), and even retrofitted a car to run on his compressed digester gas [8].

Pain's results and story were publicized in a colorful book written with his wife [9] that is available in PDF form, and a video interviewing him is available on YouTube [8]. Their claims are impressive, but have not been studied by the scientific community or

successfully replicated. Despite this, their work is notable as one of few CHR systems based on woody feedstock, which is difficult to compost compared to ordinary substrates, but contains more energy and releases it over a longer duration.

From 1981 to the present, there has been more interest and experimentation with CHR systems, many at a small scale and employing one of the above methods. In 1981 Bruce Fulford and associates formed the Biothermal Energy Center in Portland, Maine, to develop methods for heating small scale greenhouses with compost [10]. Their primary technique was forcing compost exhaust into a biofilter growing beds within a greenhouse, with the intent of utilizing the CO2 and ammonia as well as heat in the compost exhaust. However, there were issues with excessive odor, ammonia and humidity in the greenhouse.

The above concepts, while mechanically simple, have logistic and thermodynamic limitations. Heat exchangers placed within the compost are limited by the poor thermal conductivity of the substrate, and the difficulty of placing and removing them when compost is moved. Direct use of the compost or compost gases is thermally efficient, but the odors and condensing moisture that come along make it difficult to optimize.

A more viable way to capture compost heat is by passing hot compost exhaust over a heat exchanger. As compost exhaust is almost always saturated, at typical temperatures of 140 °F over 90% of the captured energy is latent heat is released by condensation on the heat exchanger surface. This is in fact occurring in all CHR systems, but more obvious when using an external heat exchanger

Agrilab Technologies Inc. (AGT), a Vermont-based company for which this author works, built its first CHR system at a heifer operation in Enosburg Falls, VT, using 60' long stainless-steel heat pipes in a 3' diameter plenum. The heat pipes are connected to a 600-gallon storage tank, and the hot water was used to heat a radiant floor in the heifer barn and temper water for the animals.

Matt Smith and John Aber (University of New Hampshire) and Robert Rynk (Cornell University) have published the most extensive study of the history of compost heat recovery, which compares the performance of many experiments and practices and is referenced here [11].

2.2. Scientific Literature:

Research and development of compost technologies has focused on efficient processing of organic material into quality compost; little attention has been paid the production and use of compost's thermal energy. There is a minimum scale at which a compost system will achieve thermophilic temperatures; for example, a "small" compost windrow of several cubic yards will have a lesser thermophilic proportion than a larger windrow of tens of cubic meters. This scale makes it difficult to experiment liberally with compost recipes and architectures.

Academic research has largely approached this issue by performing laboratory scale experiments using insulated vessels or incubators, and by building mathematical models of full scale systems. Heat production rates in ~0.2 m^3 vessels were found [12] to range from ~80-240 W/m^3. Passive convection airflow rates have been modeled based on

experiments in 105 L insulated vessels [13]. Finite volume models have been developed [14] [15] [16] to predict compost performance with high resolution in space and time, but complexities of the process are challenging and computationally heavy to model. Analytical models [14] [15] [17] describe the compost system as a whole, and are less computationally intense, but have low spatial resolution.

The most relevant research found in this review was performed by Tjalfe G. Poulsen [18], who estimated temperature and air flow in passively aerated compost piles using Kriging techniques. He measured and mapped temperature and pressure for 11 days across a passively aerated compost windrow of mixed sewage sludge and yard trimmings, out the top third. His temperature contour plots show about half of the compost pile as thermophilic as shown in Figure 2. Poulsen found that differential pressure was generally negative at the base of the pile and positive at the center, generally flowing in to the bottom third and out the top third.

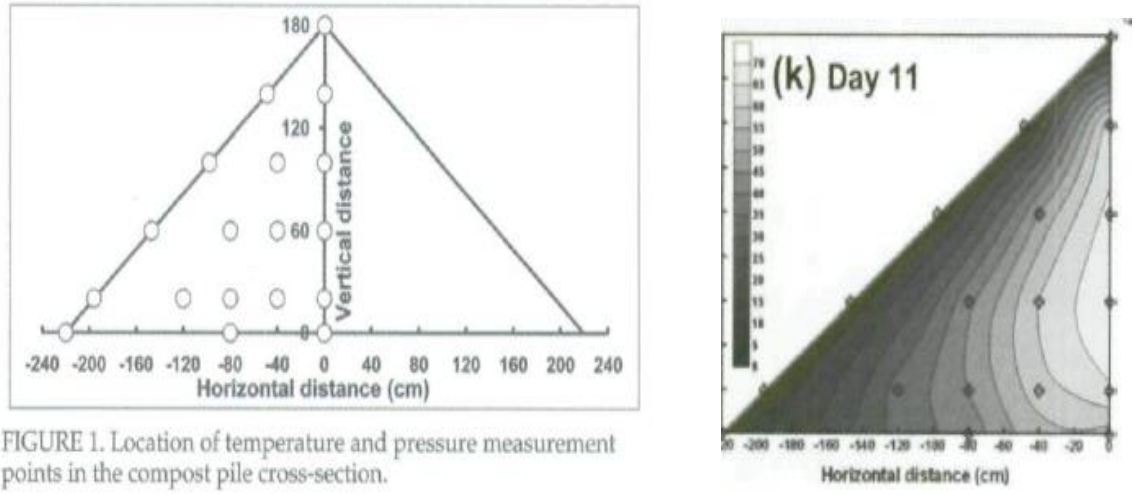

FIGURE 1. Location of temperature and pressure measurement points in the compost pile cross-section.

Figure 2: Poulsen's Kriging Results

2.3. Current Industry

Currently, the only known commercially available CHR systems are provided by AGT and Treia Technologies. Treia, founded in 2010 and based in Frederic, MD, is a mechanical engineering company that specialized in heat capture and reuse, including chiller heat recovery and solar thermal. Their *Biomass-HRS*™ is designed for the poultry industry; stainless steel flat plate exchangers placed in the chicken litter are connected by refrigerant lines to a centralized heat pump unit, and used to provide heat to the chicken houses and for wash water. It is unclear if they are currently in business as their website is down and online presence is dated.

AGT provide pre-assembled mechanical system, design and construction assistance for negative ASP CHR systems. AGT's current market focus is the dairy industry and compost businesses. A typical AGT system operates a compost pad that holds four windrows, ranging from 50 to 200 cubic yards each. Aeration pipes or channels at-grade on the pad are connected by below-grade ductwork to the aeration and heat recovery unit, which may be housed in a shipping container or barn.

A typical AGT mechanical package includes one 2 to 3 hp., 3-phase blower that is speed controlled by a frequency drive and pulls air through a plenum containing a high efficiency heat exchanger designed for the condensing and corrosive environment. Ducts coming from the compost are controlled by actuated dampers at the plenum, and the compost is usually aerated one zone at a time. AGT systems can also recirculate compost from one pile into another, which can help jump-start a cold pile or conserve heat, and be

fitted with compost heat powered drying units. Generally, water from the site is piped through the mechanical unit in a closed loop, and used to heat radiant slabs, or provide process water heat by a second heat exchanger.

CHAPTER 3: Project Storyline

Note: While most of this document is presented in the objective third person, this section is anecdotal and thus addressed from the first-person perspective. It is included as I feel it is relevant context and hopefully interesting to the reader.

3.1. Previous Work

I became interested in compost heat in 2010 when I was introduced to the work of Jean Pain by my friend Sam Gorton. At that time, I was completing a 2nd undergraduate degree in Civil Engineering at UVM. With the support of Donna Rizzo, I was funded by a Barret Scholarship to do a feasibility study on the Jean Pain concept, and we co-authored a paper on a subject. The economics were found to be somewhat compelling, particularly if the compost product was sold for $25 per yard or more, if the systems performed in the same realm as Jean Pain claimed. A significant part of my research was a geometric analysis of the compost pile; I found that even in a mound size of 50 to 100 yd^3, the volume loss of an insulating "skin" on the outside of the pile is significant even if only 6" or 1' is considered inactive. The paper was submitted to the Journal of Compost Science & Utilization, and accepted upon revision; however, I must admit I did not accomplish the revisions and moved on to other projects.

The concept of heating and producing compost with wood chips had appeal, and there was a local group of enthusiasts, the "Compost Power Network" lead by Gaelan Brown [5], that got together and attempted Jean Pain style CHR systems at private residences, and a couple at the VT Compost Co. in Montpelier. It was interesting how

enthusiastic everyone was despite the dirty work and uncertainty. However, few systems produced good results, and it was clear that not only was the methodology unclear, but the investment in plumbing to use the heat was also more significant than expected by the group. Once the pipe was buried in the pile and everyone went home, there was little that could be done if it's temperature faltered besides pour hot water on it.

Apparently I still had the bug though, as I was determined to figure out if this could work. In the summer of 2012, I invested in a used 10" capacity Valby™ wood chipper, which is an unusual brand as it can be adjusted to produce chip sizes from ¼" to 1" thick, and I modified it to go down to 1/8" cut thickness. I did help produce feedstock for a 14 yd^3 pile for a friend that summer in Brookfield, which did not get hot and she was disappointed to say the least. However, the following summer it was much rainier, and the pile then heated provided warm, if not hot, water to her outdoor shower all summer as intended.

That December (2012) I conducted my first experiment, generously hosted by Dave Whitney / EcoSolutions LLC where I was working at the time, by filling a 6' diameter, 8' tall fiberglass cylinder with fine chip from the Valby set at 3/16" diameter. In preparation for the experiment, I was looking for a solution to measure many temperatures affordably and came across the Web Energy Logger™ (WEL), sold online by Phil Malone at www.ourcoolhouse.com. The WEL uses a 1-wire™ bus (developed by Dallas-Maxim) to which at least 50 1-wire™ temperature sensors can be wired. Rather than conventional sensors that use an analog signal, the 1-wire sensors are pinged every minute by the WEL, and reply with their unique ID and value. This system has been integral in the viability of

the research herein, as it would be many times more expensive to purchase conventional data loggers with so many temperature points, and quite difficult to run 50 to 100 separate wires to the terminals.

The "Chip Chimney" experiment at EcoSolutions reached a peak temperature of 143 °F fifteen days after loading, on December 25th, and subsequently cooled off to a high of 100 °F by late January. Only about 20% of the vessel even reached thermophilic temperature – it was probably not watered well enough and over-exposed to draft as it was set on a pallet for aeration. However it was a valuable learning experience in many ways. That spring (2013) I enrolled in the Mechanical Engineering M.S. program, and reprocessed the data in Donna Rizzo's Geostatistics class, where I learned the techniques and began the code used in this current research.

In 2013 I was also involved as a contractor in two student lead compost heat projects that were funded by the UVM Clean Energy Fund. The first (in January) was a Jean Pain style mound intended to heat the student greenhouse at Slade Hall, which involved improvement to the greenhouse and installation of a hydronic root-zone heating system, as well as construction of the mound. The mound was about 40 yd^3 of fine wood chips, bark mulch, sheep manure and wood-shop sawdust, with straw bale sidewalls and perforated 3" polyethylene drain tile beneath for aeration. Students coiled 600 feet of 1" polyethylene pipe into the mound while it was built with a payloader operated by physical plant staff. Once the system was built, the plumbing system was pressurized and there was a leak in the pipe coil (probably due to trauma from my compost thermometer!), which had to be dug out, found, patched and rebuilt. Despite all this effort the temperatures

unfortunately never exceeded 122 °F; this was making the fragility of the Jean Pain style systems clear.

That summer (2013) I contracted with another UVM Clean Energy Fund project, which became a 3-sided hemlock bay at the UVM Horticulture Farm, measuring 16' wide by 12' deep and 10' high, with the exhaust piped into an adjacent greenhouse to a biofilter growing bed. Bruce Fulford was involved in the project as a consultant, and the system was based on his previous work with New Alchemy and the Biothermal Energy Institute. 3" polyethylene drain tiles on grade at the bottom of the bin connected to an inline fan in the greenhouse, which pushed air into the growing beds. Unfortunately, the pipes weren't properly pitched, and they became filled with water. We then built a condensate sump and ran the system through the winter, but it never produced noteworthy heat output.

I met Brian Jerose, owner of Agrilab Technologies Inc. where I currently work, during the design phase of the Horticulture Farm project, and he hired me shortly thereafter. It has been a great job in many ways, not least as it is my subject of interest, and it initially accommodated my student schedule. As work picked up, I spent more of my time on AGT projects and my student work slowed down, which is why it has taken five years to complete the course requirements and thesis project. Over the years we have improved the design of AGT systems with state of the art control and monitoring systems, and developed compact, highly efficient mechanical packages that include speed controlled blowers, zone control, recirculation and drying functions. The units are built by AGT with custom parts provided by local metal shops (Mtn. Air Systems and Giroux Fabrication). They generally operate four compost zones of 50 to 200 yd^3 each, and fit onto a 4' x 8' steel skid or in a

20’ shipping container. We have also designed and helped build several CHR systems, most recently and notably at Vt. Natural Ag. Products in Middlebury.

3.2. MS Research

This thesis was proposed to the committee in the spring of 2014. Upon encouragement by Dr. Hitt, I successfully applied for an EPSCOR 2014-2015 SBIR phase 0 grant which funded most of the project expenses. My friend Dan Heyde generously allowed me to conduct the work in a barn on his farm in Moretown.

The grant award was received in late fall 2014, and in early winter I began building the project. After designing and fabricating the system, I ran power and internet about 400’ through the farm and installed the necessary wiring and lighting in the barn space. Cold temperatures and the process of building the data / control system took additional time, and the experiment was initiated in early April 2015.

The experiment was successful in that it produced hot compost as well as lots of high quality data. However, I was unable to get the compost uniformly hot, as the aeration would force cold ambient air into one side of the system. Also, while there was clearly heat being produced, the exhaust rarely achieved useful temperatures. To address this, I built an air manifold with 2” pneumatic valves that can recirculate or aerate upwards or downwards through the vessel, but I was unable to run the experiment during my thesis period. The 2nd round platform is fully set up at my house in Richmond and ready for compost, and I hope to run it and apply the techniques developed herein very soon.

CHAPTER 4: Experiment

4.1. Vessel

The compost vessel was designed to be built from common construction materials and insulated enough to be autothermal during cold ambient conditions. In large compost systems convection and radiation are assumed to dominate heat loss, and in very large systems forced aeration is required to cool the compost [3]. In small vessels, however, conduction becomes increasingly important. Figure 3 shows a simple calculation of conductive heat loss by a cubic compost vessel assuming a uniform mean temperature difference across the insulation surface and an R value of 2.28 W/m^2/K (equivalent to 2" rigid polyisocyanurate insulation). This would be equivalent to mean compost surface temperature of 35 C with exterior temperatures ranging from -35 to 30 C. Compost heat production has been generally estimated to range from 100 to 250 W/m3. Based on this it seems safe to say a cube of 1 m^3 or greater should perform well even in cold temperatures if air flow is controlled effectively.

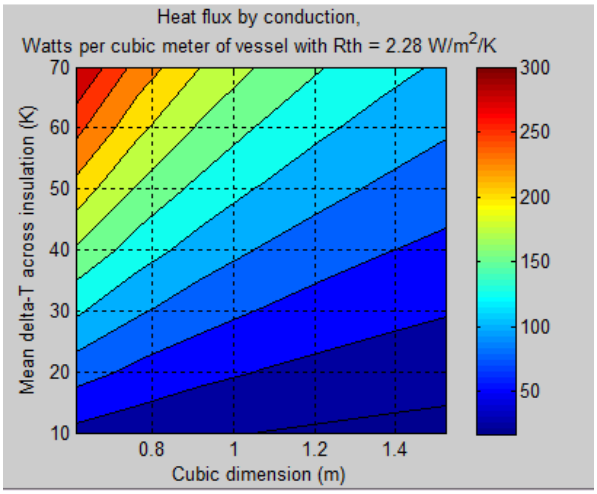

Figure 3: Simple conductive heat loss

The vessel is a cube built of 4' x 4' (half sheets) of 2" rigid foil-faced polyisocyanurate insulation (Dow "Tuff-R 13"). The panels are screwed to an internal frame of 1.5" x 1.5" lumber with plastic insulation washers, and the edge joints are capped

with 3” aluminum trim to avoid rodent damage. The system sits on a hemlock pallet, and the edge joints are sealed with foil tape during startup. Figure 4 shows is a CAD drawing of the vessel with front and right panels removed, and a translucent 6” layer of wood chip over the aeration manifold.

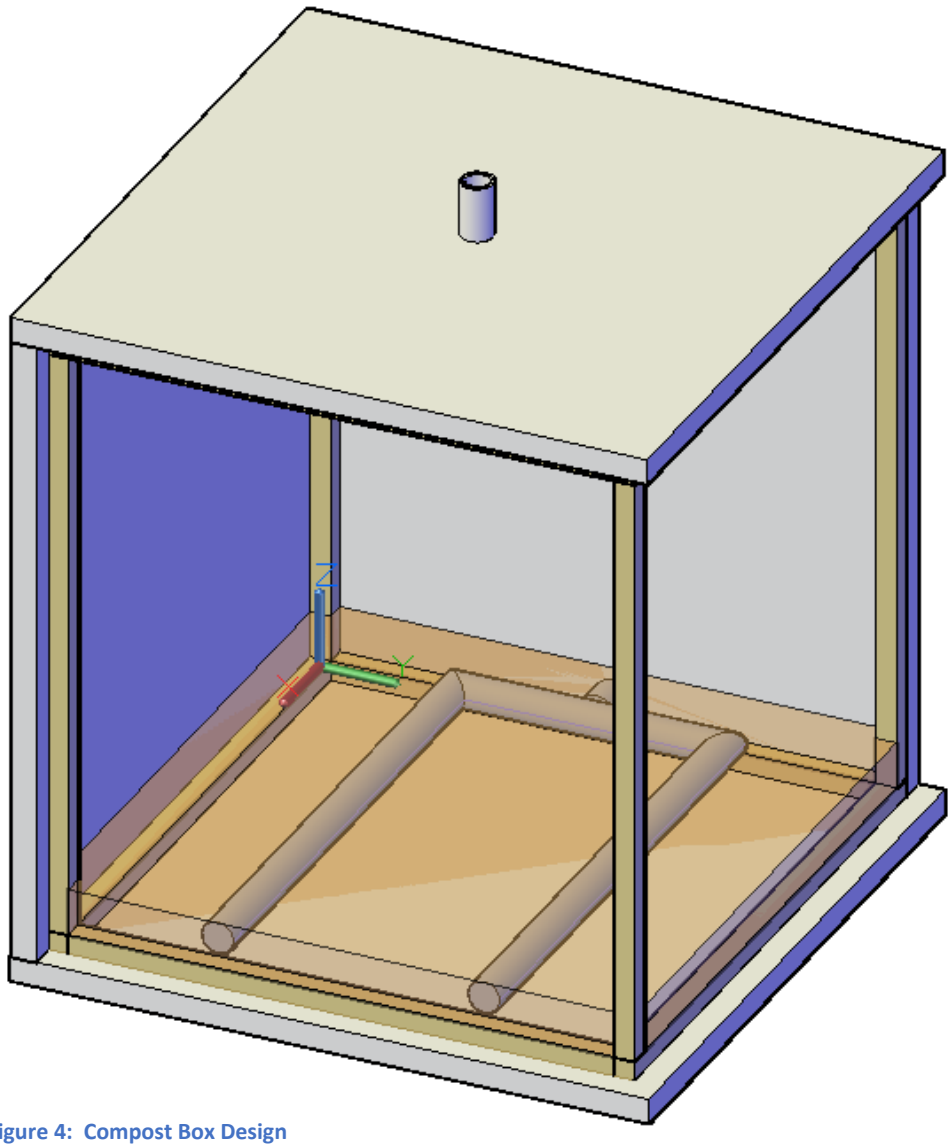

Figure 4: Compost Box Design

The aeration manifold comprises 2-legs of 2” PVC pipe, each drilled with ½” perforation every 3” at +45° and -45° from downward. This is a total of thirty-two ½”

perforations as seen in Figure 5. The perforations are held back 11” from the walls to reduce channeling along the edges of the compost.

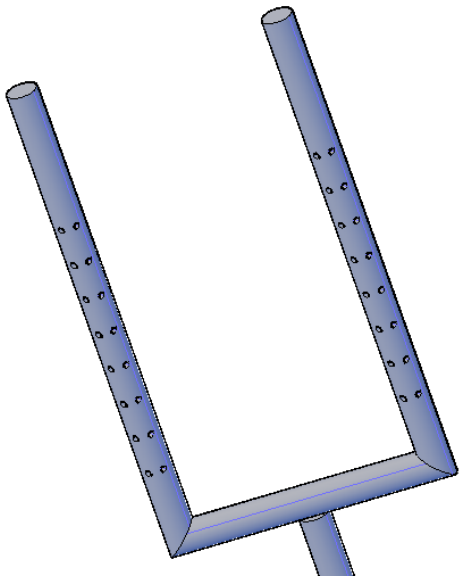

Figure 5: PVC Aeration Manifold

Forced aeration was provided by a 25.3 W Dayton PSC Blower, with a flow range of 51 to 23 CFM (at 0.5” static pressure). Flow was calculated by measuring static pressure across the blower and comparing to the manufacturer provided fan curve (attachment). The blower was attached to the bottom manifold header outside the vessel wall. The top air outlet was a short piece of 2” PVC pipe fastened and sealed at the center of the top insulation panel. To prevent passive air flow when the blower was off, a weighted damper was built with a foam rubber seal, and actuated by a large 110V solenoid during aeration.

4.2. Data and Controls

4.2.1. Brief description

Data was generated by a bus of eighty-four 1-wire™ temperature sensors (81 in the compost vessel plus ambient, top outlet, and bottom outlet), plus a pressure sensor at the blower inlet. This data was collected by two Web Energy Loggers (each handling a portion of the temperature sensors) and posted at 1-minute intervals to the www.welserver.com website.

A CLICK C0-10ARE-D programmable logic controller was used to control fan cycle times, and to convert the pressure signal from 4-20 milliamps to 0-5 V input to a WEL analog terminal. Pressure signal was generated by a Dwyer MagnaSense™ MS-121-LCD differential pressure sensor.

While the WEL values can be read remotely, the CLICK model used is not ethernet enabled; thus, for remote operation (to adjust the blower cycle times) a small laptop was left on and connected to the PLC, and run using remote desktop software.

4.2.2. Detailed Description

The data and control system (D&C) is housed in a 16" x 24" fiberglass NEMA-4X enclosure that was salvaged from an unrelated project. Figure 6 shows the D&C with the original components plus some additions for future work, as noted. Data logging was performed by the two Web Energy Logger (WEL) units [19]. The WEL is a low-cost HVAC monitoring system with a Rabbit™ RCM3700 CPU core. Each WEL can accept an array of 1-wire sensors (described below), two 0-10V analog signals, six pulsed inputs and 8 switch closure inputs. The WEL is configured in a web browser interface through the local area network (LAN) to upload readings to the host website at www.welserver.com, which it does once per minute. The data is logged and easily downloaded from the website; however, as the WEL does not have on-board data storage, interruptions in internet connection can cause data gaps.

1-wire temperature sensors were used, which contain a DS18B20 temperature sensing chip in the probe tip, which soldered to a wire lead and encapsulated in potting compound. Most sensors used had stainless steel jackets as shown, while some were covered only with potting compound. The reseller specs (attached) claim accuracy of +/- 0.5 K (0.9 R) at -10 to 85 °C which is in the range of the experiment. My personal trials

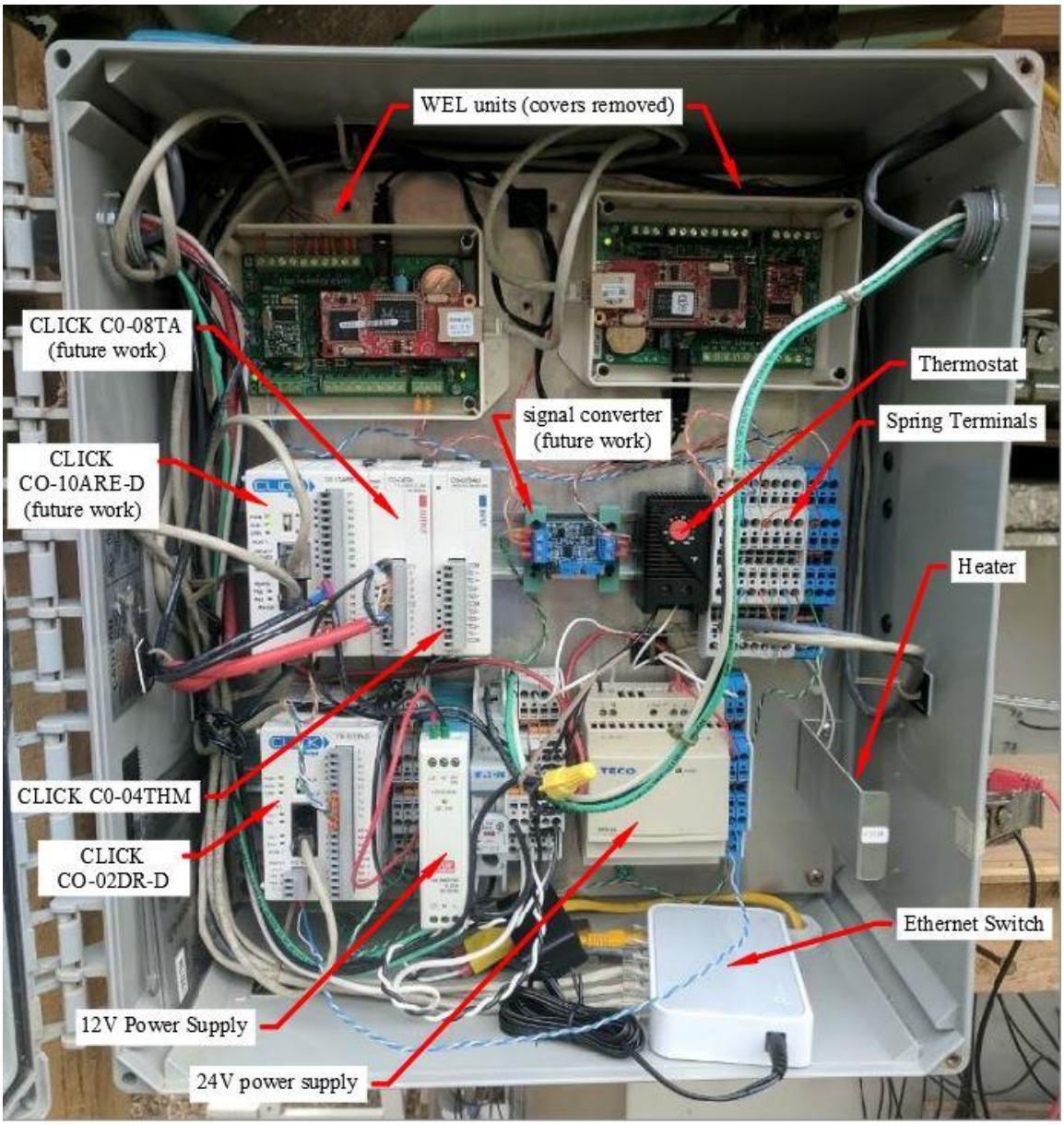

Figure 6: Data & Control System

in 2013 (on sensors purchased at that time) found them to be more accurate, generally within 0.5 °F when calibrated in ice-water or hot water.

To build a 1-wire bus with the WEL, sensors are added individually and then named using the "Scan Bus" procedure. Each sensor has a unique 16-digit alphanumeric ID which is then associated with its name. Once sensors are labeled and names stored in the WEL memory, they can be used in any configuration if they are connected in parallel, with the correct polarity, along a shared wire "bus". The WEL pings the 1-wire bus every minute, and the sensors respond with their ID's and values. This works quite well unless the signal is degraded by sensor interference, or electronic noise from another source.

To avoid interference, the ideal 1-wire bus architecture is a single twisted pair wire with each sensor branching off at regular intervals. Additional branches, hubs, and sensors in the bus increase the likeliness of a bad reading. However, with large numbers of sensors in one spot, the ideal architecture is impractical, and the bus ran through a series of hubs (jumped spring terminals) mounted to the experiment. With the WEL, there was no relevant limit to the size of the bus, just increasing likeliness of failed reads. Phil Malone recommends no more than 55 sensors be connected to the WEL in an ideal arrangement, thus two WEL buses were used to split the array of 85 temperature sensors.

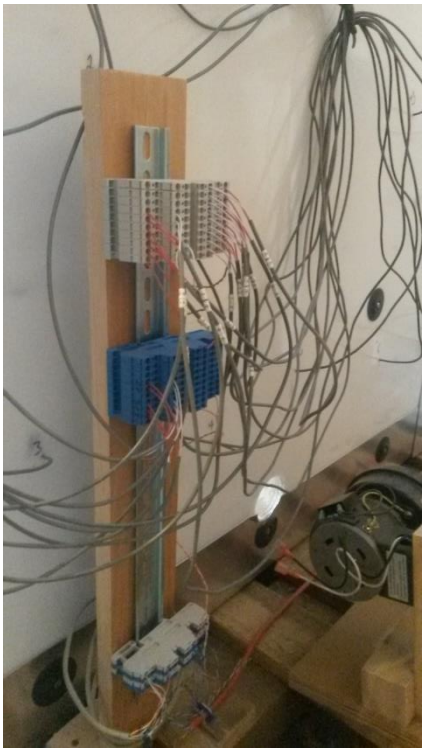

Figure 7: 1-Wire Bus Terminal

The capabilities of the WEL 1-wire bus enabled the large number of temperate points measured. There are some disadvantages, most significantly that if the bus is shorted, or internet connection interrupted, all measurements are lost. Occasionally a troublesome sensor can increase failed readings without completely shorting the bus. Fixing this requires the ability to troubleshoot the sensor array if needed, by the process of elimination. To aid this troubleshooting, the sensor hubs of jumped spring-clamp terminals were arranged in groups with jumper wires that could be adjusted. This did come in handy, as there were problems with some sensors in the array over time that could be addressed more easily.

The 1-wire bus terminals of each WEL were used for a portion of the temperature points. One 0-10V WEL input was used to receive the pressure signal from the blower, which was produced as a 4-20 milliamp signal and converted to 0-5V by the PLC. The pressure was measured and transmitted by a Dwyer MagnaSense™ MS-121-LCD differential pressure sensor, with ¼" polyurethane tubing connecting one port to a hole in the side of the pipe by the blower, and the other left open to atmosphere.

4.3. Operation

4.3.1. Startup

Figure 8: Sensors Taped to Bottom of Compost Vessel

Once the experiment was in place, the D&C system was started up and sensors, which had been pre "named" and labeled in the office, were carefully added to the inner vessel walls at prescribed locations by drilling holes though the vessel walls for sensor leads, and taping sensors to the walls in their prescribed locations.

Next the PVC air manifold was placed in the vessel and covered with a 3-1/2" layer of fine wood chips. The more permeable chip layer helps even out pressure to provide more even aeration at the compost surface. The front panel was fastened to the frame, and outer panel joints sealed with foil tape. Compost was supplied by VT Compost Co. courtesy of Karl Hammer; Karl's "hot mix" was used, which is a mixture of half composted product (manure, food and "winter bark") mixed approximately 50% with fresh winter

bark. Compost was added by hand, stopping to place arrays of sensors at the prescribed layers. Compost was filled to a 44" depth, creating a 44" cube of compost (1.81 yd^3) with a 1/2" headspace at the top.

4.3.2. Operation

Compost was loaded on April 7th, 2015. As data logging began before the compost was loaded, the actual composting period began on day 7 of the monthly logged data file. Initial aeration rates, based on standard composting practices [2] and the blower rate of about 35 CFM, was set at 6 minutes per hour. At first the blower was set to inject air into the bottom of the compost. This caused the bottom of the vessel to remain cool as it did not re-heat between aeration cycles. Aeration was adjusted to 2.5 minutes every 40 minutes on April 8th. On April 9th, as sensor #52 placed in the bottom center of the compost was still only 53 °F, the blower direction was switched to pull from the bottom of the box. This did produce more even temperatures though the top portion became relatively cool, and the box coincidentally heated rapidly.

The short aeration bursts did not achieve usefully hot outlet temperatures, and on April 10th, the fan cycle was changed to 10 minutes every 2 hours, then 10 minutes every 3 hours to address that. This produced higher outlet temperatures, but also caused the compost to cool rapidly.

On April 13th, the aeration rate was reduced and compost temperatures rose. Aeration pulses were kept short until April 28th, and the measured temperatures peaked on the 18th and began to tail off. On the 28th the rate was increased, and there was a slight

positive temperature response, but then the temperatures trended towards ambient around May 1st.

The experiment was later disassembled on July 28th, and the compost had settled 3.75” since the initial loading.

Figure 9: Compost Vessel Opened After Experiment

CHAPTER 5: Data Analysis

5.1. Introduction

5.1.1. General Methodology

The first goal of this data analysis is to quantify the temperature and heat loss from the compost vessel. A second goal, which is nearly as important, is to examine the data qualitatively to check that the results are plausible, and find additional insights, such as the affects of the operating temperatures and aeration rates on the compost temperatures.

Graphical outputs were used extensively to visualize the results, and apply filters when appropriate. In general, results were plotted either as 2 dimensions as temperature or heat flow over time, or as 3 dimensional visualizations of temperatures at one time. With so many time steps involved, movies were generated from the 3-dimensonal data; while difficult to program, these were most valuable in comparing the plausibility of compost temperatures produced by various methods.

Virtually all the data processing was performed by writing Matlab™ code, while also using Microsoft Excel™ and AutoCad™ to verify and compare results.

5.1.2. Heat Flow

Heat production by the compost is measured by adding the net flow of heat from the vessel, as diagrammed in Figure 10. The net enthalpy loss (q2 – q1) is calculated using air flow, temperatures and saturation. Conductive heat losses (q3-q7) are calculated using the internal surface temperatures of the vessel, R-value of the insulation, and ambient temperature (T_∞).

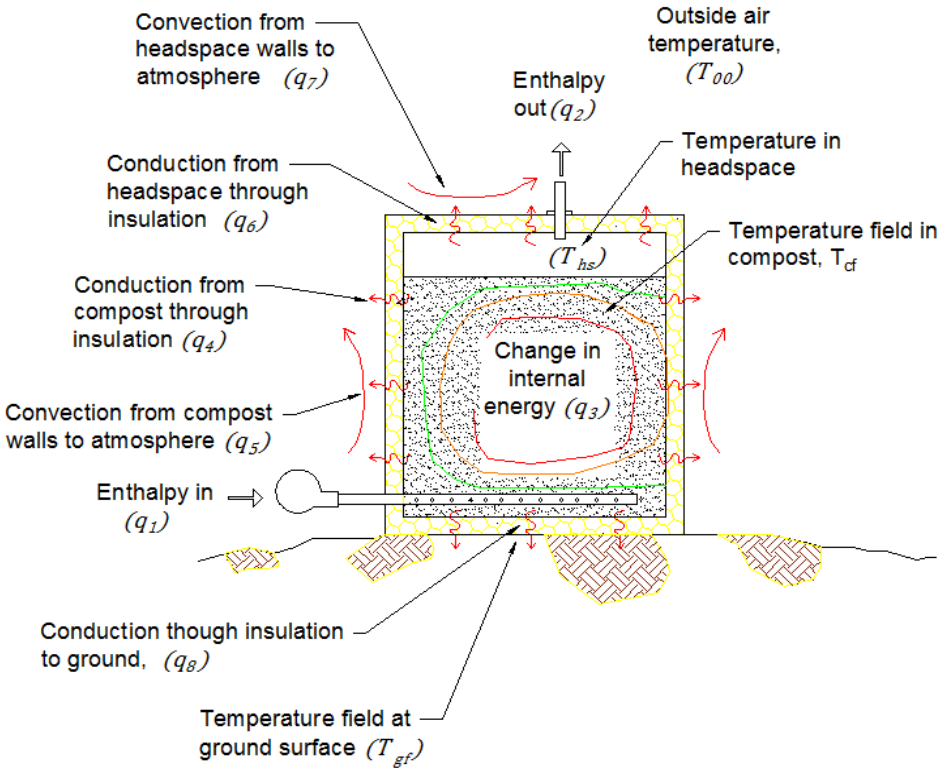

Figure 10: Heat Transfer and Temperature Fields

The change in internal heat energy (q3) is found by multiplying temperature change by specific heat capacity, C_p. C_p of compost is expected to vary significantly with ingredients, moisture content, density etc. which complicates the calculation. Since the goal of this project is to calculate the excess heat released by the compost, (q3) is not calculated here. It is a relevant operating parameter, to frame the expected compost

temperature change with heat extraction, and could be estimated in reverse using these results.

As compost temperature varies in space and time, the most difficult and interesting problem is estimating temperature across the compost volume and surfaces. In this research, the temperature fields are estimated by Kriging where irregularly spaced sample points can be used to produce a regularly spaced field of estimation points. The estimated temperature points are then applied to volume and surface area grids to calculate the conductive heat loss, and compost temperature by volume.

5.2. Initial Data Processing

The first step in analysis is to import and process the data. Data from the two Web Energy Loggers (WELs) was downloaded from the website in monthly files with unique timestamps. These were concatenated and co-indexed into one array of 111 measurements per minute over the project period of 70097 minutes, filling in missing sample times with NaN (not a number) values; a plot of all these values over time is shown below in Figure 11. Sensor numbers were then matched to their locations, XYZ coordinates for those in the compost vessel and descriptive locations for the rest (inlet, outlet, ambient temperatures, blower pressure sensor) and these verified against project notes, expected patterns etc.

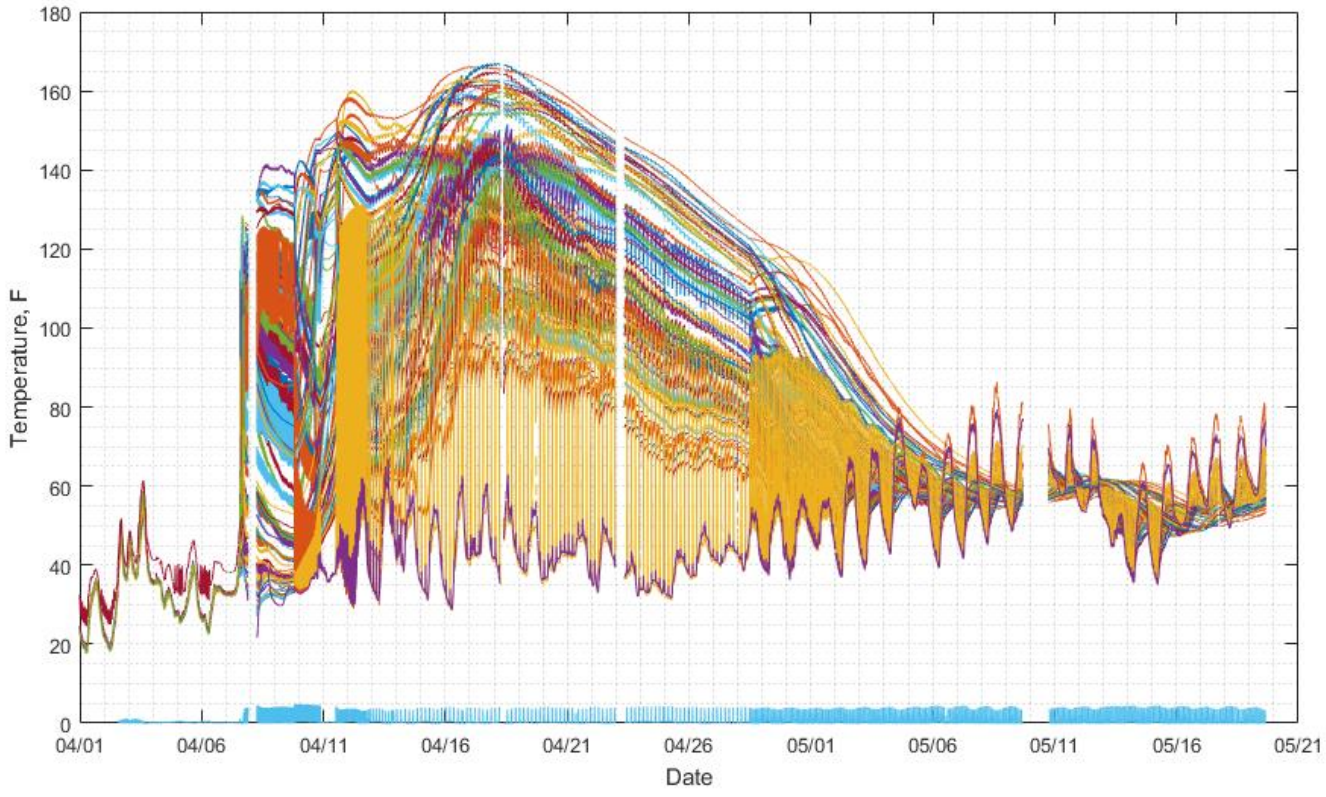

Figure 11: Raw Data vs. Time

Approximately live 81 sensor values (depending on measurement time) were captured per minute. As Figure 9 shows, it is impossible to decipher more than the most basic trends at this resolution. To confirm the locations of the external sensors, they were plotted independently (Figure 12).

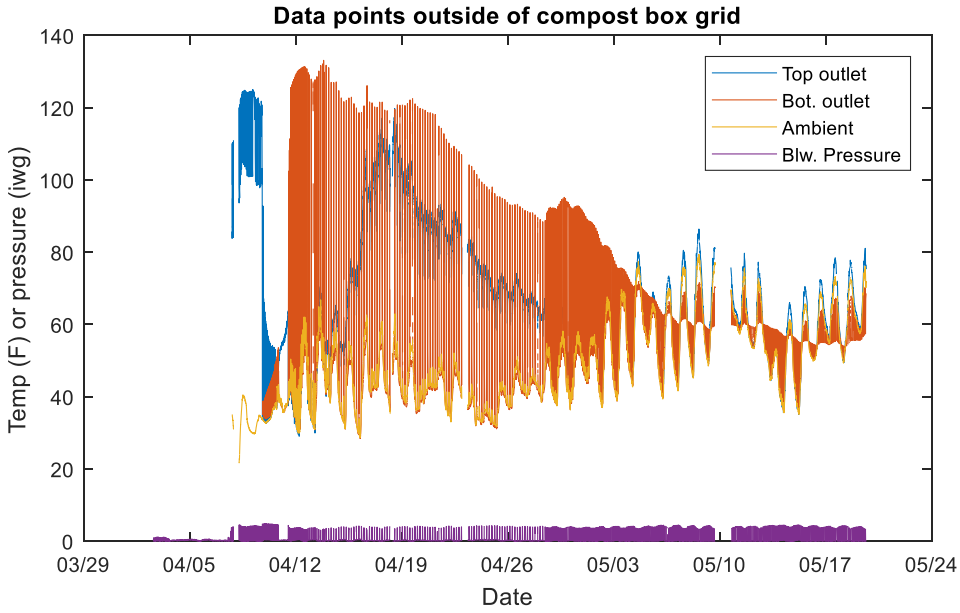

Figure 12: External Measurements, Full Time Span

Zooming in to a shorter time span, as shown in Figure 13, paints a clearer picture. You can see when the blower turns on, it pulls hot air from the compost past the bottom outlet sensor, while the top outlet is cooled by incoming air. It seems there is mixing occurring at the top outlet, as it doesn't approach the ambient temperature. Also, the ambient temperature seems to heat slightly be

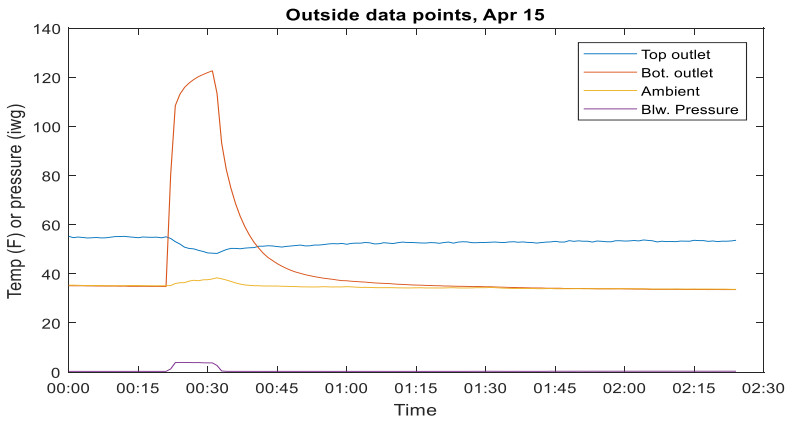

Figure 13: External Measurements, Selected Time Span

the compost exhaust, which is interesting. Neither of these phenomena should significantly affect the results.

The compost box sensors were examined with scatter plots as shown in figures 14 and 15. This allows a basic check of whether the locations and temperatures are reasonable, although only one step can be examined at once.

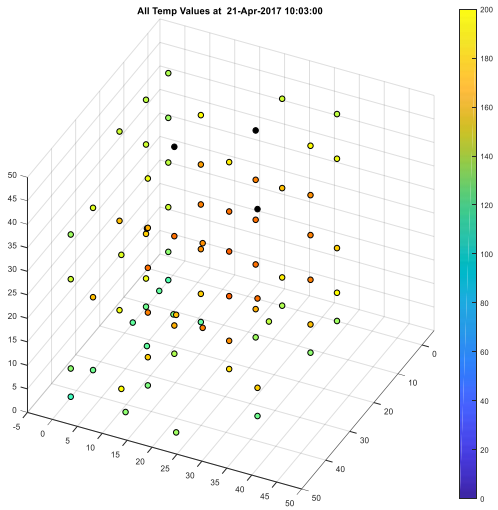

Figure 15: Scatterplot of Sensor Locations

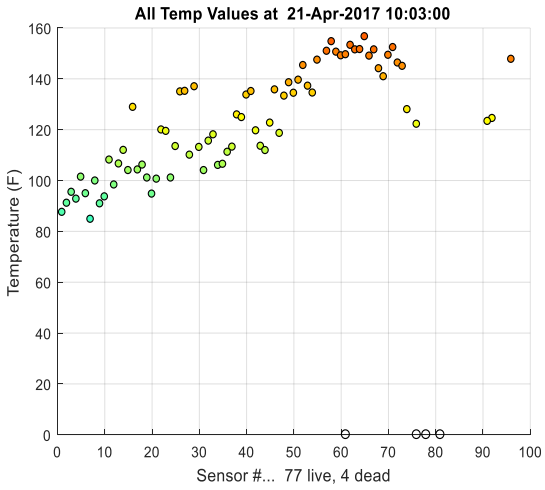

Figure 14: Sensor Temperatures, by Sensor Number

5.3. Symmetry

5.3.1. Initial examination

With reasonably uniform compost and a horizontally square vessel, one would expect the temperatures to be relatively symmetrical. Assuming symmetry helps simplify the model, but it also introduces uncertainty. Symmetry was first examined statistically by changing the pair distance measurements (described in section 5.4 below) to a combination of Z coordinate and horizontal distance from center. This did improve correlation although it still fell apart at distance, which likely come from the vertical distance as well as the effect of corners.

Better correlation was achieved by simply reflecting all sensor values over the X and Y axis, and comparing the values. This technique was also used to create virtual data points where reflected values occur and a functioning sensor did not exist. Reflected values are helpful, in this case, to bound the temperature field, otherwise Kriging can produce artificially high values on walls without sensors, as without neighbors they are statistically closer to the hot center sensors.

Sensors counts were 23, 9 and 4 on the Y=0, X=0 and X=44 walls (the floor had 20 sensors). Thus the Y=44 wall accepts the most reflections. The biggest difference at symmetry (7.4°) was found in the vessel floor at 11" from both walls. The second and third largest differences (4.1° and 3.9°) was also found 11" from walls, at Z = 33.5 and Z = 6. The largest difference found at a wall surface was 3.0°, while the average difference at the walls was 1.6°.

5.3.2. Further examination

After the initial examination of symmetry, the data points were reflected as described and added to the data set, to run the first Kriging model. Heat calculations were performed, and results generated. However, upon further observation of the data, it was realized that the initial symmetry analysis was somewhat flawed, and second analysis was enacted. This was done by first normalizing the X and Y sensor locations as distance from the walls. In this case, as the walls were 44" wide, for each point p these distances were:

$$x_{w,p} = 22 - abs(22 - x_p) \; ; \; y_{w,p} = 22 - abs(22 - y_p)$$

The vector of coordinates $[x_w, y_w]$ was then sorted by columns to produce a normalized distance from walls as walls regardless of orientation,

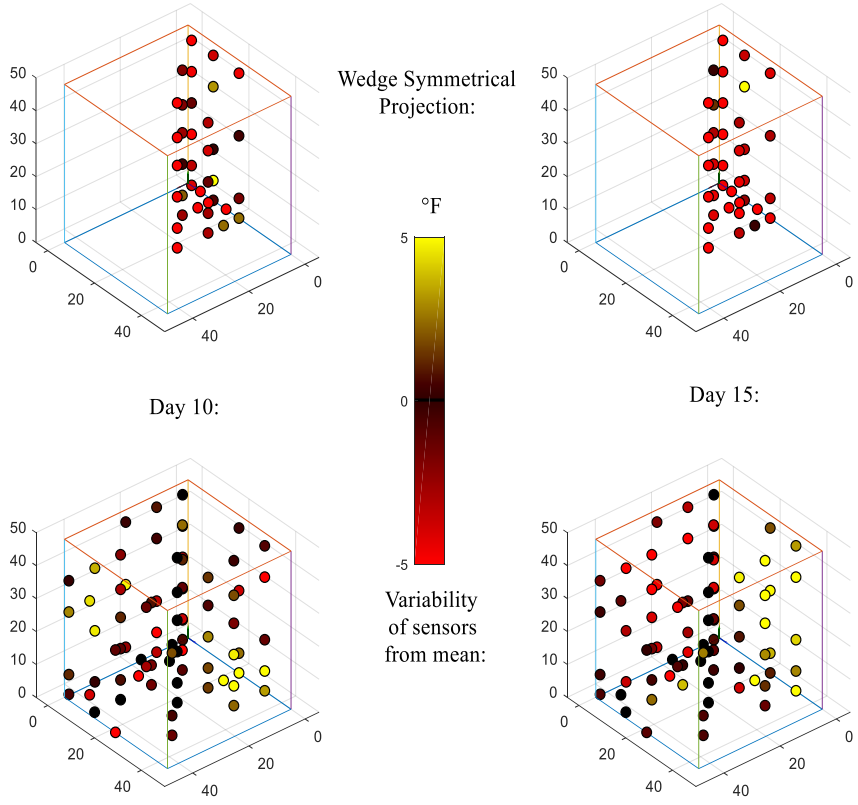

Figure 16: "Wedge-Symmetrical" Comparison

$$[w_{1,}\, w_2, z] = [\min(x_w, y_w)\,, \max(x_w, y_w)\,, z]$$

Figures 16 shows 3-D scatterplots of the "wedge-symmetrical" points, and scatterplots of the original sensor set color coded by variation from mean. Analyzing symmetry in this way produced 39 bins of matching coordinates which range from 1 to 4 sensors in each. With greater number of bins and bin counts, temperatures were more variable than initially thought, which somewhat invalidates the initially assumed symmetry. Figures 17 and 18 show a plot of departure from bin mean for all sensors over time, the second zoomed in for visibility. While most of readings are within 3 degrees of the mean, significant outliers are seen.

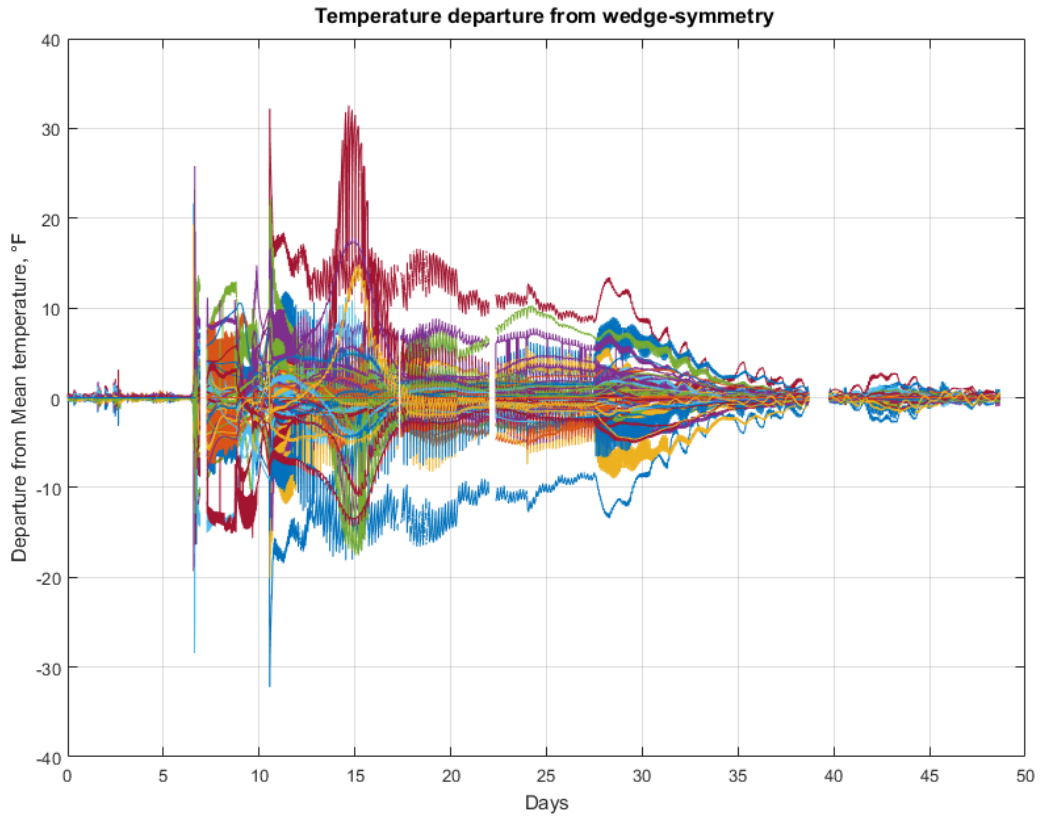

Figure 17: Wedge-Symmetrical Temperature Departure

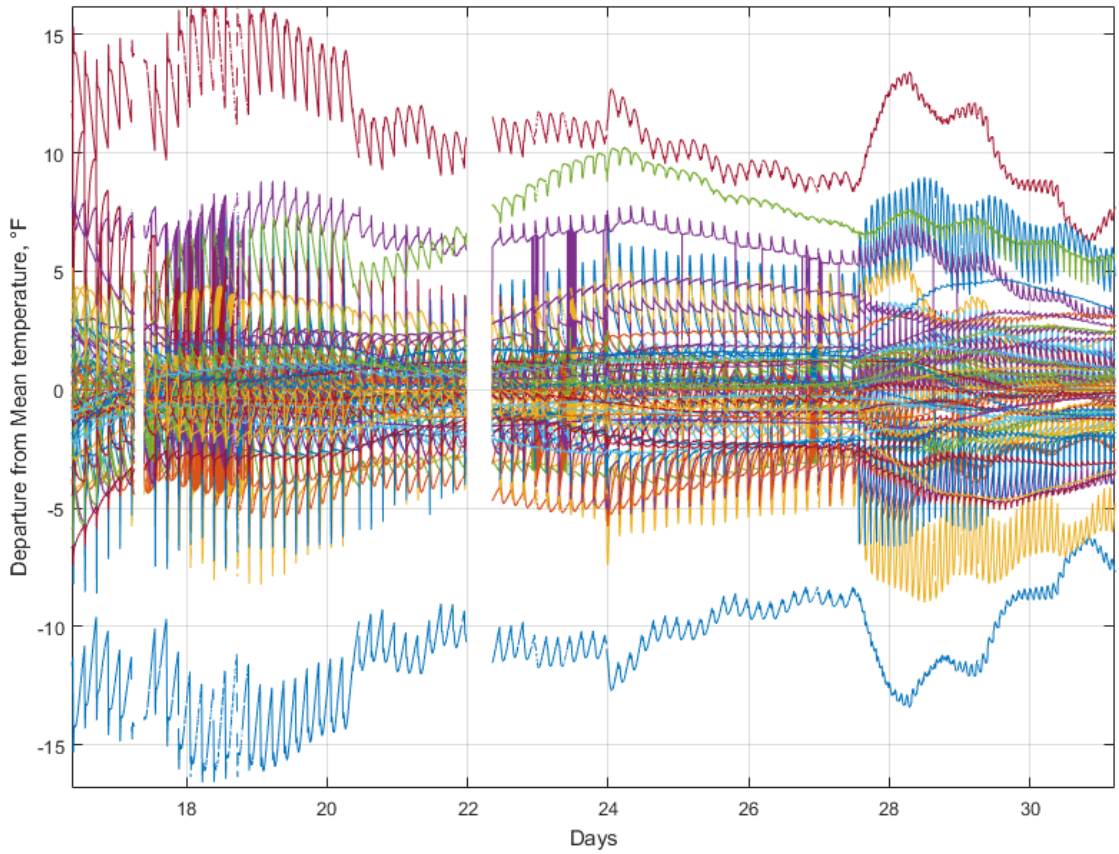

Figure 18: Wedge-Symmetrical departure, zoomed in

5.4. Kriging explained

Temperatures in the compost and at the insulation surfaces were estimated with the geostatistical technique called Kriging. The field of Geostatistics was developed largely by the mining industry to estimate underground resources with a small number of sample points. In addition to the expense of geological sampling, it often unfeasible to sample in an even grid over a large area due to constraints such as property rights, topography, etc. Thus, point-to-point interpolation is not usually applicable, and another method was sought.

The first Kriging step is to statistically compare all samples to one another by comparing each point to every other point in the data set. To do so, a 2-dimensional array of samples is constructed with each dimension containing values of all samples. With *n* samples, an *n x n* matrix of "sample pairs" is made. The covariance matrix [C] compares the variance between each sample as $\sqrt{(T_i - T_j)^2}$. The distance matrix [D] contains the measured distance between each sample pair, which may be the normal (shortest path) distance, or it can be weighted or otherwise constructed; regardless of distance manipulation, the resulting [D] matrix will contain one-dimensional pair distances values.

Next the variogram (scatter plot of data pairs by distance and covariance) is examined, and model is fit to estimate variation by pair distance. The raw variogram is generally a cloud of points, data points then are "binned" by combining pairs within certain distances of each other and re-plotted until correlation patterns emerge. A model curve is fit (visually and/or statistically) to the binned variogram. Figure 19 summarizes this process. Viable models include "linear", "spherical", "exponential", "Gaussian" and "cubic" functions. Each function has parameters called the "nugget' (the Y axis intercept), "sill" (maximum Y value), "range" (X value at the sill), and "Lambda" for linear and spherical models. As it has been fit to the data, the chosen model is considered the best estimation of the variance over space between any sample pair, and is then used to prescribe the variance between unknown points and the known data set.

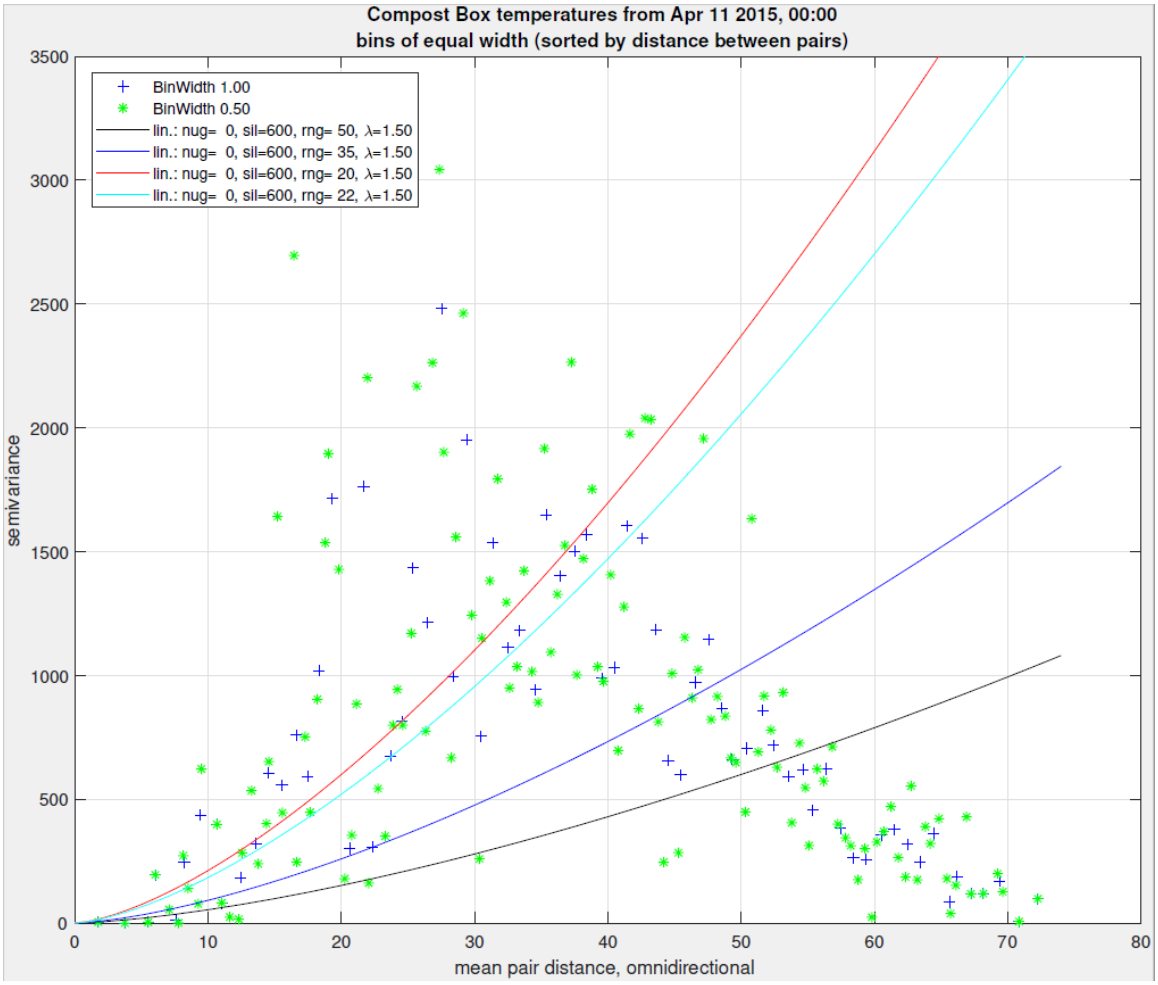

Figure 19: Vairogram

A domain of desired estimation points (typically a 2-d or 3-d grid) is generated, and estimation distance [F] and covariance matrices [G] are generated with methods similar to [C] and [D] except in this case, the pairs are each estimation point compared to each sample point. Thus, if there are *m* estimation points and *n* sample points, *m x n* matrices are produced. "Sample" matrices [C] and [D] are square and symmetrical across the diagonal, which is comparisons of samples to themselves and thus all ones for [C] or zeros for [D]. "Estimation" matrices [F] and [G], however, are not symmetrical or square; there are typically many more estimation points than sample points, thus $m >> n$ producing a tall matrix.

The next step is to generate a weighting vector $\boldsymbol{w}$ for each estimation point, which is indexed to all sample points. Programmatically this is accomplished with linear algebra, by adding a row and column of ones to the ends of [C] (called $[C_2]$ here) and, in a loop, generating $\boldsymbol{w}$ for each sample point by matrix inversion of $[C_2]$ by the row of [G] for estimation point *m*, with a one at the end. For example, the weighting of sample *m* is calculated as:

$$\boldsymbol{w}_m = [C_2] \setminus [\, G_{m,1} \ldots G_{\text{-man},} \, 1]$$

The estimates for each point are then generated by the sum of all sample values multiplied by $\boldsymbol{w}$, for example the temperature T at point *m* given sample values $\boldsymbol{V}$ is:

$$T_m = \text{sum}(\, \boldsymbol{V} * \boldsymbol{w}_m \,)$$

In effect, the value of each estimated point is a weighted sum of all the known values, with the weighting a function of the modeled variation over distance.

5.5. Kriging the sample data

Variograms were analyzed at various time points (representative of different compost ages, temperatures and ambient temperatures) to find a satisfactory covariance model. Typically, 77 sensors were active at any time, producing 250 temperature values after reflection, yielding 31,250 data pairs per variogram. Covariance functions were found visually with with code that allows the user to try multiple bin and model selections (Figure 19). After several trials (including the initial Kriging), linear, spherical and Gaussian

models were selected for comparison, with the following parameters. A nugget of one was used for the Gaussian model to prevent matrix inversion issues.

Linear: Sill = 1200 ; Range = 30 ; $\lambda = 1.4$

Spherical: Sill = 400 ; Range = 100

Gaussian: Sill = 400 ; Range = 50 ; Nugget = 1

5.5.1. Initial Kriging:

In the first Kriging analysis, all sensor values were reflected across the X and Y axes, as described in section 5.3.1. The temperature fields were then analyzed at representative times, using the linear model with ranges between 35 and 50, and with estimation grid resolutions from 10 to 20 points (2.31" to 4.88" grid spacing) in the X, Y and Z directions. Little difference was found in the results; the models with resolution of 10, 15 and 20 usually took 0.3, 2.1 and 11 seconds to run respectively. Processing time did vary somewhat, which may be due to the number of active sensors at that time, or the computer's state. Occasionally the code would fail, probably due to a minute when few or no sensors reported data.

To model the temperature field over the full experiment time, a resolution of 15 x 15 x 15 and 2-hour time steps were chosen after some trials. Steps that yielded errors were omitted programmatically. This model ran successfully in around 30 minutes. The maximum, minimum and mean temperatures were compared (shown in Figure 24, section 6.2). The maximum temperature was closely correlated with the Kriged maximum, while

the mean was higher which is to be expected, since there were more sensors on the relatively cool walls. The minimum Kriged temperature was above the measured minimum for some periods, particularly between 15 to 27 days, which is when the compost was hottest. This may be due to the somewhat coarse grid resolution, or other factors to be explored, but it is notable that the departure of the mean and minimum values is somewhat concurrent.

5.5.2. Subsequent Kriging:

The initial Kriging produced plausible results of heat transfer and mean compost temperatures. However, 3-dimensional examination of the temperature field showed it was implausibly symmetrical, due of course to the reflected mean values. This lead to the second symmetry examination. It was decided to abandon the sensor reflections, and model smaller portions of the domain for comparison. Domain resolution was generally set at 2" spacing. The Kriging code was made more efficient, and filtered to skip time steps with less than 5 live temperatures. This dramatically reduced model time, to range from around 0.3 to 2 seconds per time step. Various time steps were used depending on comparison goals. Some of the larger time models were 35 days at 1-hour steps, (840 steps) and 1 day at 1-minute steps (1440 steps).

The linear, spherical and Gaussian models were compared over domains of the full box, half box (Y <0 22") and quarter boxes (Y <= 22", X >= 22" or X>= 22"). Average temperatures, heat losses, and 3-dimsional temperature maps were compared between models.

5.6. Heat Calculations

Heat production was calculated as the sum of heat loss from the compost vessel. This included conduction through the walls and floor, and forced convection when the blower was running and damper was open.

5.4.1. Conduction

To calculate the conductive heat loss, the temperature fields at the inner insulation surfaces were calculated by applying surface areas to each Kriged temperature point. The inside of the compost vessel was 44 inches on a side, so with a grid of 15 points, the grid spacing was 44”/14 = 3.14”. In this case an area of 9.87 in^2 was applied to each temperature point, then the area of those on the sides were divided by two the corner points divided by four. The manufactured R-Value of the insulation is 13 ft^2 * °F * hour / BTU; this was multiplied by 3.41 (Watt/(Btu/hr)) to yield 44.33 ft^2 * °F / W. The conduction was then found at every temperature point by:

$$Q_p(W) = A(in^2) * \frac{ft^2}{1728\ in^2} * \frac{(T_p - T_\infty)°\mathrm{F}}{R = 4.33 * °\mathrm{F}/W}$$

5.4.2. Compost Temperature

Compost temperature was calculated using a finite volume method, where each temperature point was assigned a volume; at a 15-point grid resolution, the volume is (44”/14) ^3 = 31.04 cubic inches per point, for those fully in the compost volume. Points on the side walls were adjusted to half the volume, edges to one quarter, and corners to one

eighth. The temperature volumes were then binned at 1-degree intervals and combined to yield the total volume of compost at each temperature.

5.4.3. Convection

Heat loss by aeration (forced convection) is calculated by the net enthalpy loss. This requires knowing the mass flow of the air, it's temperature and humidity entering and leaving the vessel.

The air flow rate of the blower, in cubic feet per minute (CFM), was calculated by first modeling the manufacturer supplied blower curve using Matlab's *fit* function as shown in Figure 20. The spline fit was chosen as it is simpler and more conservative, as the static pressures were generally around 0.35 iwc (inches water column).

Blower signal processing is shown in Figure 21. As the pressure signal and the blower curve have an indirect relationship, the signal was bifurcated at 0.06 to remove the floor. This left the ends of each pulse with an artificially high reading, which was indexed (red dot), and assigned half of the nearest CFM value.

Specific volume and specific enthalpy of the air were found similarly, using chart data from the "Moist Air Properties" chart from the Engineering ToolBox website, available at https://www.engineeringtoolbox.com/moist-air-properties-d_1256.html. The chart data was coverted to use degrees Farenheit with metric units of density and energy, and curves were fit as shown in Figure 22.

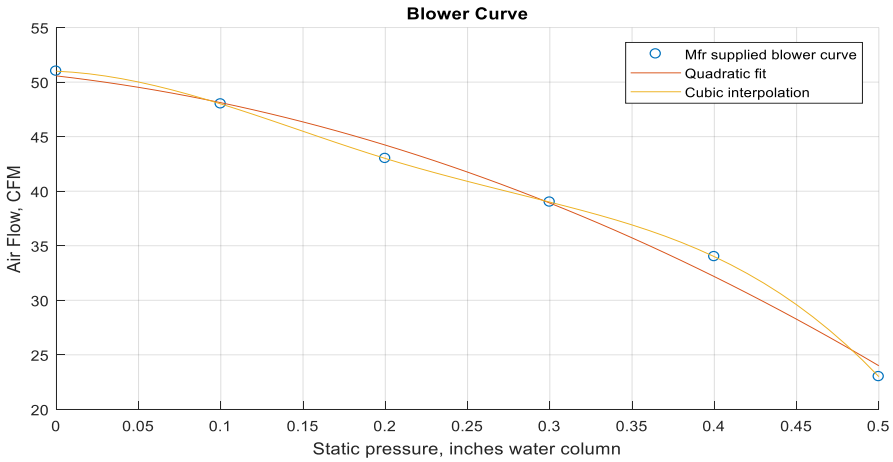

Figure 20: Blower Curve

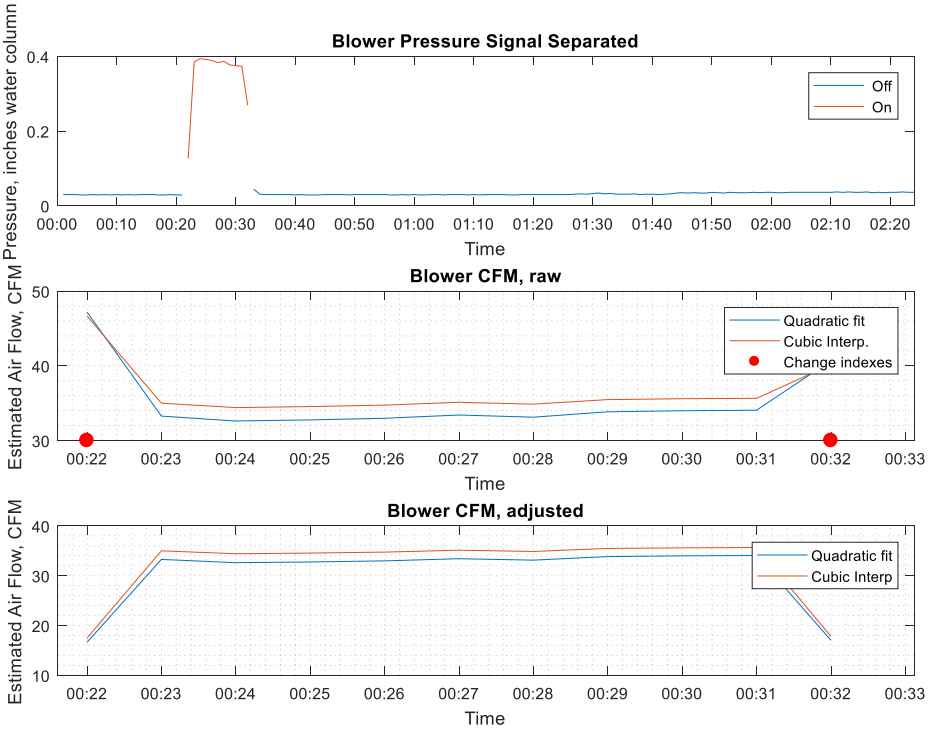

Figure 21: Blower CFM Signal

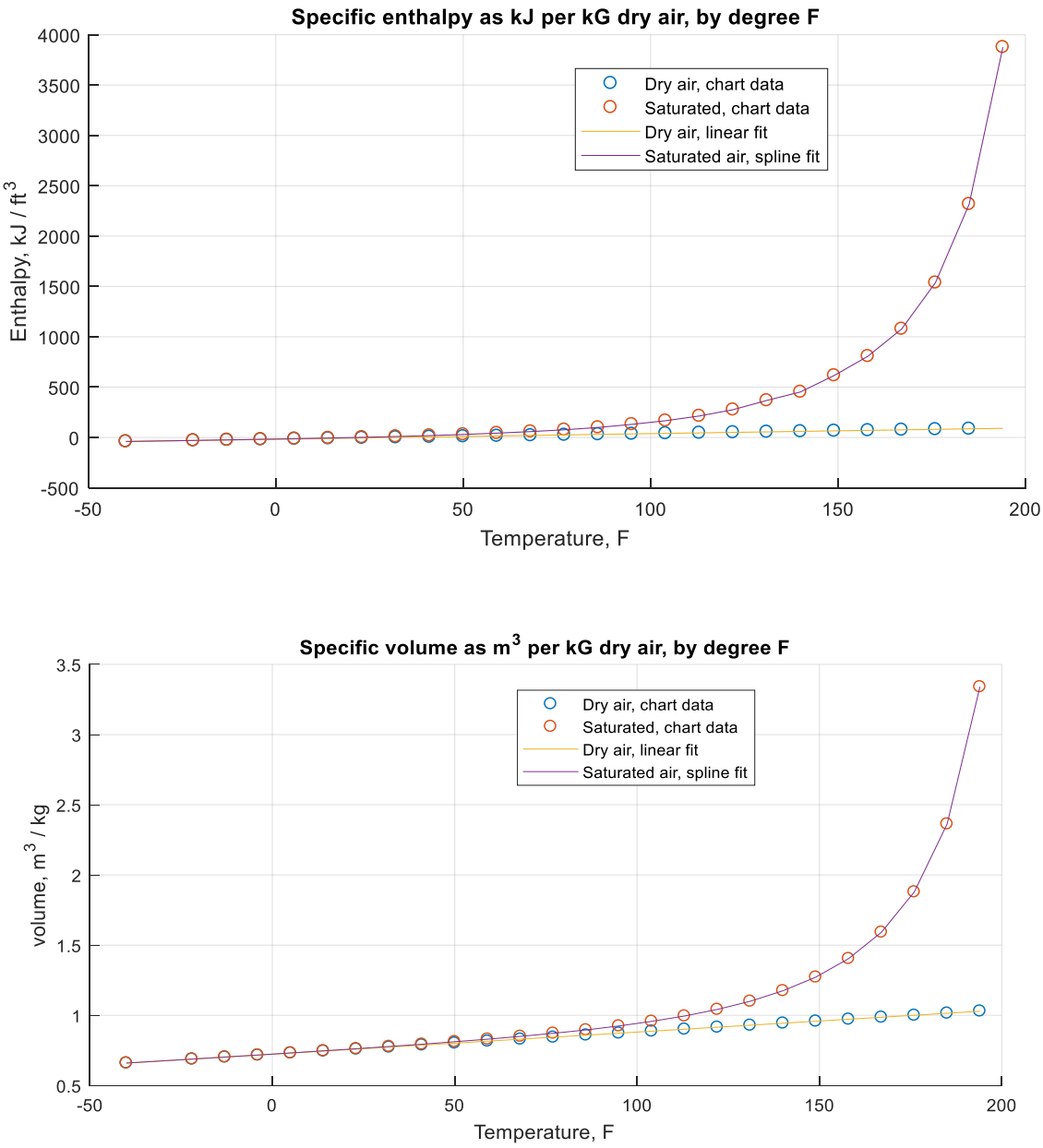

Figure 22: Specific Enthalpy and Volume of Dry and Saturated Air.

With these processes in place, the convection enthalpy is calculated by:

$$h(W) = Q\frac{ft^3}{min} * \frac{m^3}{35.315\ ft^3} * \frac{1}{v(°\text{F})\frac{m^3}{kG}} * h(°\text{F})\frac{kJ}{kG} * \frac{1000\ J}{kJ} * \frac{min}{60\ sec}$$

where $v(°\text{F})$ and $h(°\text{F})$ are the specific volume and enthalpy as functions of °F. To simplify the process, the incoming cold air is assumed to be dry while the compost exhaust is assumed to be saturated. If the compost is performing well, saturated exhaust is a safe assumption. While the ambient air had some humidity, as it was generally below 50 °F this difference has little relatively little effect. An aeration pulse with measured temperatures and associated enthalpy flow is shown in Figure 23.

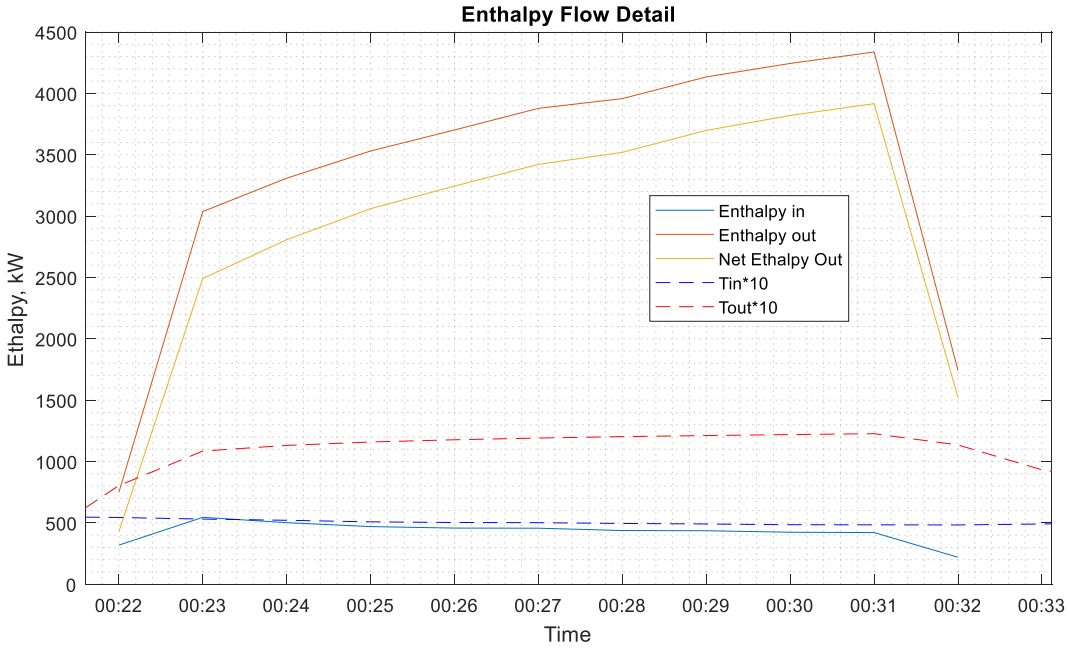

Figure 23: Enthalpy Calculation

5.7. Filtering Results

Fluctuations due to sensor fails or missing values lead to extremes or gaps in the results. Sensor noise from the system could be described as low frequency and high amplitude; more directly, the sensor reads were usually accurate and stable, but occasionally an extremely outlying data point was generated. More commonly, some or all the sensors would fail to report, leading to gaps in the data. Filtering of enthalpy calculations is described above in section 5.6.

All Kriged results were sensitive to missing sensor values, leading to relatively rapid temperature field changes. While models with relatively large time steps (on the order of 12+ hours) did not always require filtering, smaller time steps captured more outlying results. These were filtered using the rate of change of the mean domain temperature as an indicator. At each time step, the change rate was calculated by the difference between the step mean temperature and the moving mean of surrounding values. At steps where this difference was above a chosen filter level, the temperature field from that step was removed (converted to NaN). After experimentation, a moving mean of 15 hours with a filter removal of > 9° F was found to satisfactorily remove extremes while preserving data trends.

Missing temperature values, due to failed sensor reporting or from filtering, were filled in using linear interpolation. Other methods (cubic, *inpaint_nan*) produced nice looking results, but tended to fabricate local extrema; the linear mean has the added benefit of indicating large data gaps to the reader, as the temperatures normally fluctuated.

Chapter 6: Results & Discussions

6.1. Convective Heat Loss:

Enthalpy loss occurred during aeration, in pulses of minutes, ranging to above 5000 Watts. This is difficult to observe over the experiment period, and the average enthalpy over time is of greater interest. Thus, enthalpy output is processed with repeated moving averages to create a curve that is meaningful in comparison to compost temperatures, shown in Figure 24.

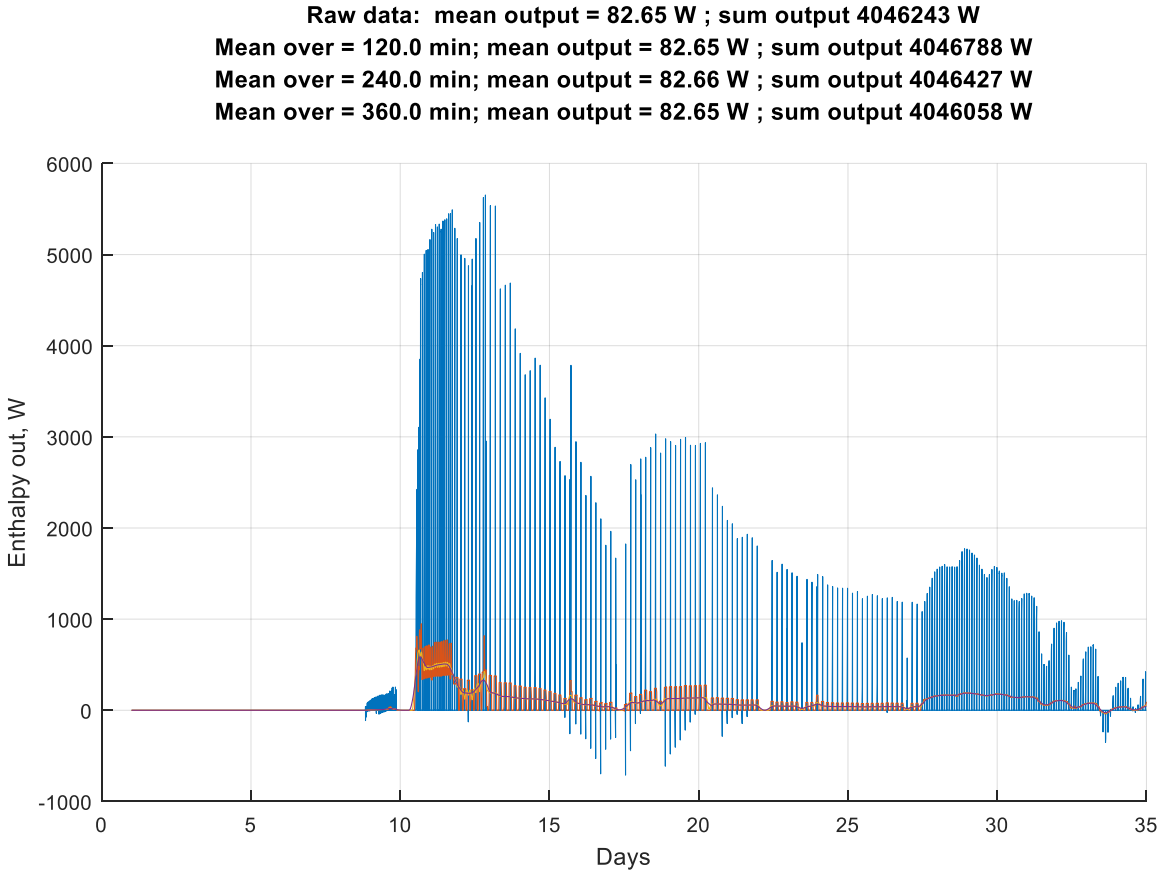

Figure 24: Convective Heat Loss Processing by Moving Average

It is important to note that the enthalpy loss does not directly represent useful energy per a CHR system. To estimate the useful enthalpy from the compost, one would

have to compare to a use temperature and efficiency. Since the outgoing temperatures in this experiment were rarely above typical use temperatures, the useful energy was not estimated here, but could be done with the same methodology as the total enthalpy calculations.

6.2. Conduction & Combined Heat Loss

As described in section 5.4.1., calculating conduction from the vessel walls requires estimating the temperature fields at the walls, done here by Kriging. The temperature in the compost was quite variable, and different Kriging models used produced some variance in the compost temperature fields. This is particularly of interest in gauging how much of the compost was thermophilic, as discussed in the following section. The temperature at the walls did exceed 140 degrees at the hotter periods, but was less spatially variable than the internal compost temperatures; due to this and the high density of sensors at the vessel

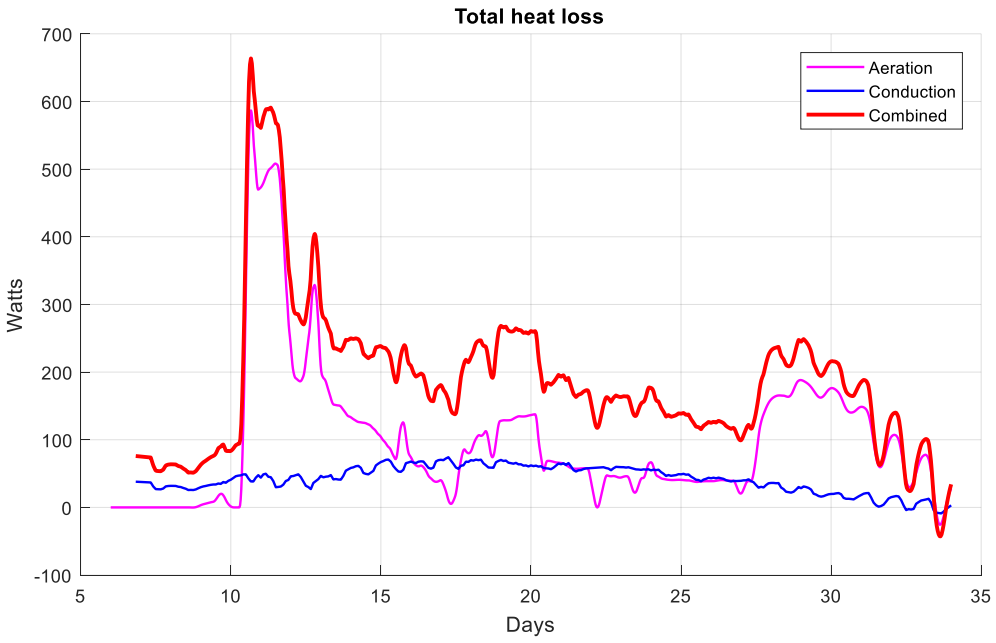

Figure 25: Combined Heat Losses

surfaces, conduction was generally similar between all models. Figure 25 shows heat loss from convection, conduction, and combined heat loss vs. time.

6.3. Kriging & Compost Temperatures

While the heat loss results were generally consistent across all reasonably behaved model, the compost temperature fields were much more variable. To compare these, step-averaged results can be compared over time in 2 dimensions, or the temperature fields at various time steps can be visualized and compared. While 2-dimensional plots are useful to compare overall model results, to inspect why (or where) model outputs varied it is necessary to visualize the temperature fields in more detail.

In time series plots, the simplest comparison is the median (volumetric mean), minimum and maximum temperatures. Figure 26 shows the initial Kriged results compared to the sensor values. More advanced time series plots can be produced by sorting and binning the volumes of compost by temperature, and plotting as a contour over time.

Various ways of visualizing the temperature fields per step time were developed, including 3-dimensional slice plots, contour plots of domain slices, and 3-dimensional plots of the temperature surfaces with transparency. Movies of multiple such sub-plots were generated to visualize and compare the temperature field results over time.

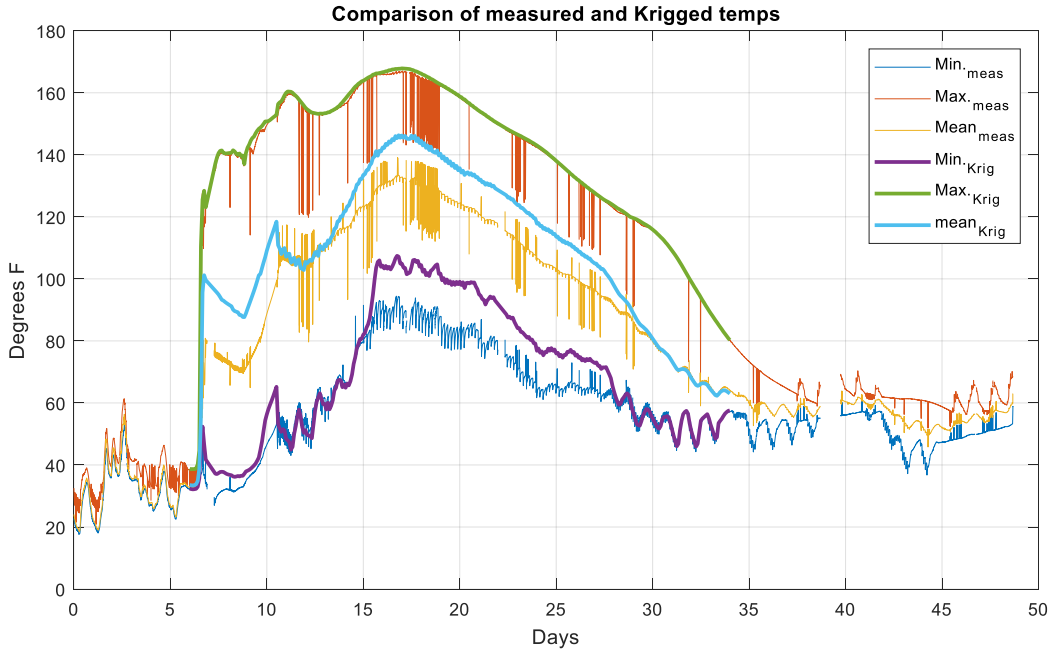

Figure 26: Comparison of Kriged and Measured Temperatures

The selected linear, spherical and Gaussian covariance models were compared over a range of domain and sensor selections. Three covariance models were compared, over four domain options, over various sensor selections, each producing upwards of 10 plotted results. With the number of permutations and plots per model, it is neither feasible nor appropriate display all comparisons examined, so only selected plots are shown here.

The temperature volumes, in addition to being visually interesting, are important to assessing how much of the compost is thermophilic, and thus heat producing, at a given time. The "specific power" of the compost is defined here as the amount of heat produced by the active portion of the compost; determining how much of the compost is "active" is a qualitative simplification at this point, but it is related to the thermophilic portion of the compost. While the overall heat release varies little by model type, the specific power is much more sensitive.

The half box (Y <0 22”) domain, shown in Figure 27, has the highest sensor density and is thus considered the most accurate. The following figures compare average temperatures, heat losses, volume temperature, temperature volumes, and specific power and accumulated heat calculated by the three models on the half domain.

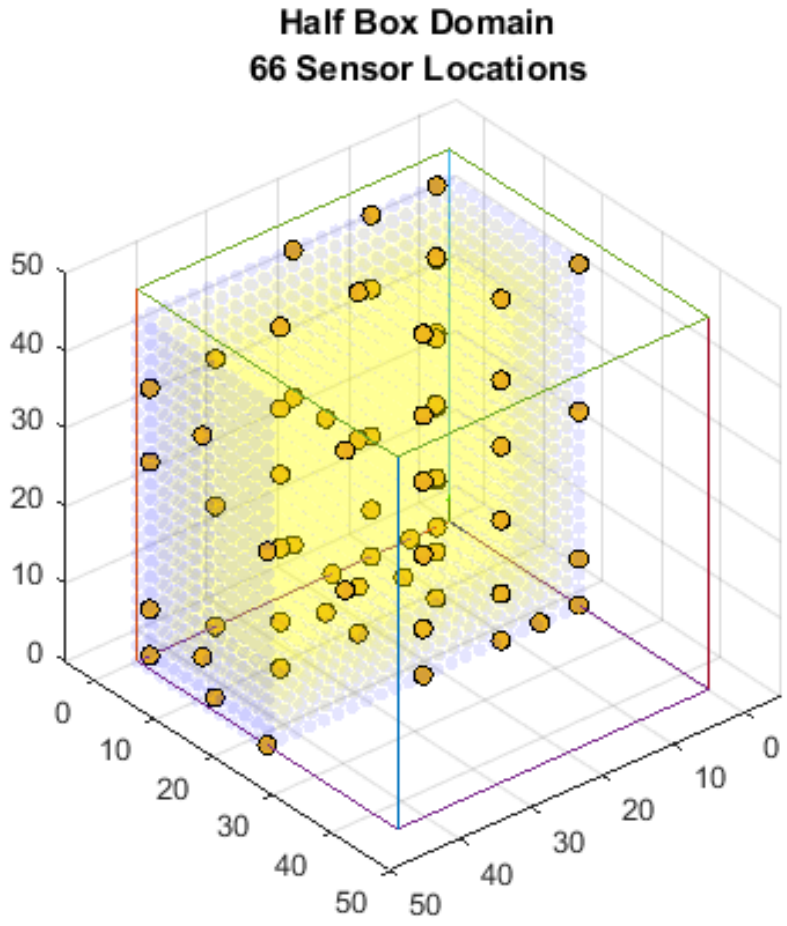

Figure 27: Half Box Domain

Figure 28 shows maximum, median, and average surface temperatures calculated by each model, and the resulting heat losses, which are similar. As seen, these values are generally similar except that the Gaussian model has higher maximum temperature; this does cause a minor increase in conductive heat loss around day 9.

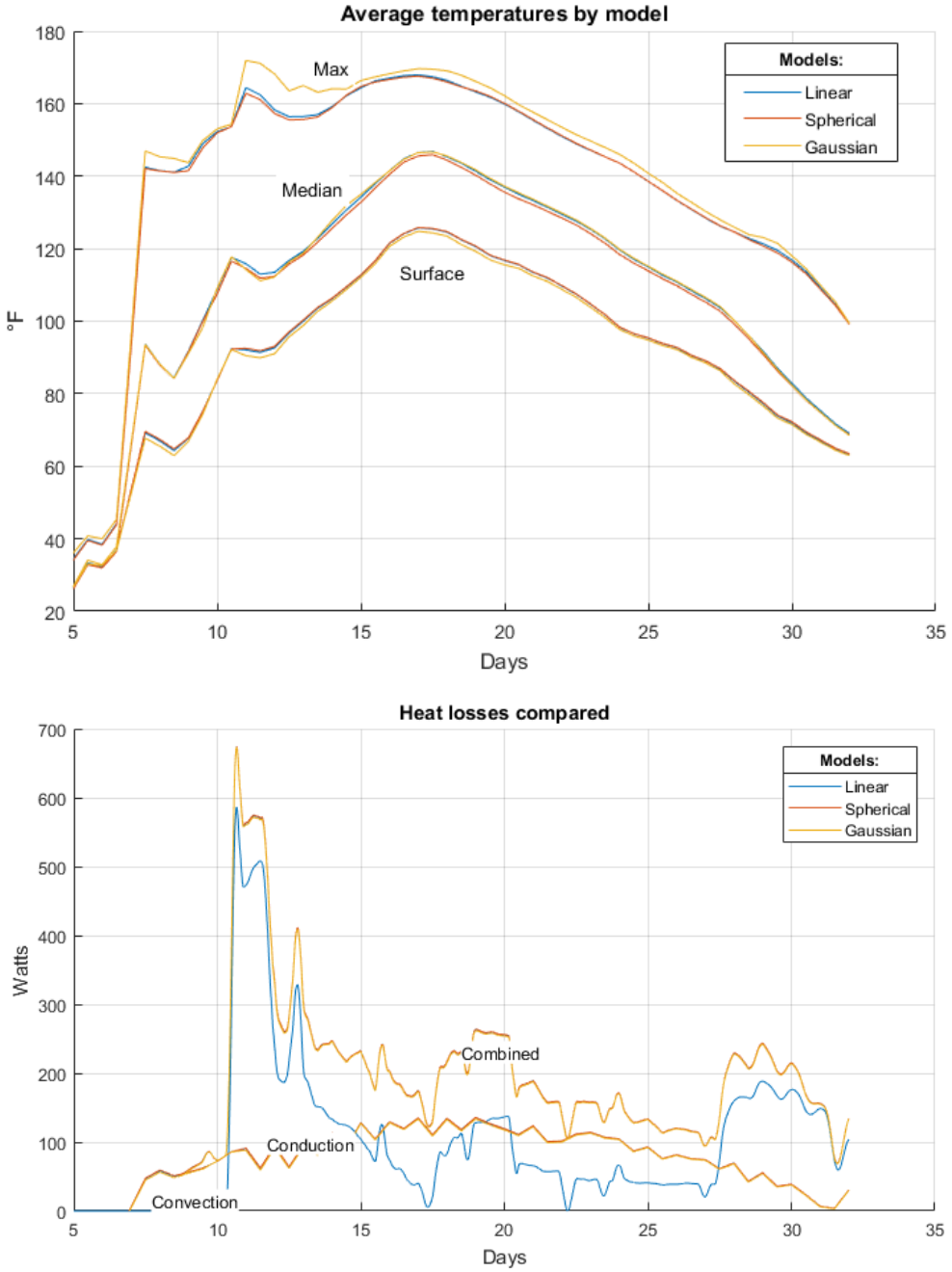

Figure 28: Average Temperatures and Heat Losses Compared

Figure 29 shows the "volume temperatures" (amount of compost at or above a given temperature) and "temperature volumes", which is conversely the minimum temperature of a volume bin. The bottom lines in the temperature volume comparison shows the minimum compost temperature of the entire volume, while lines the top is that of the hottest 0.2 yd^3.

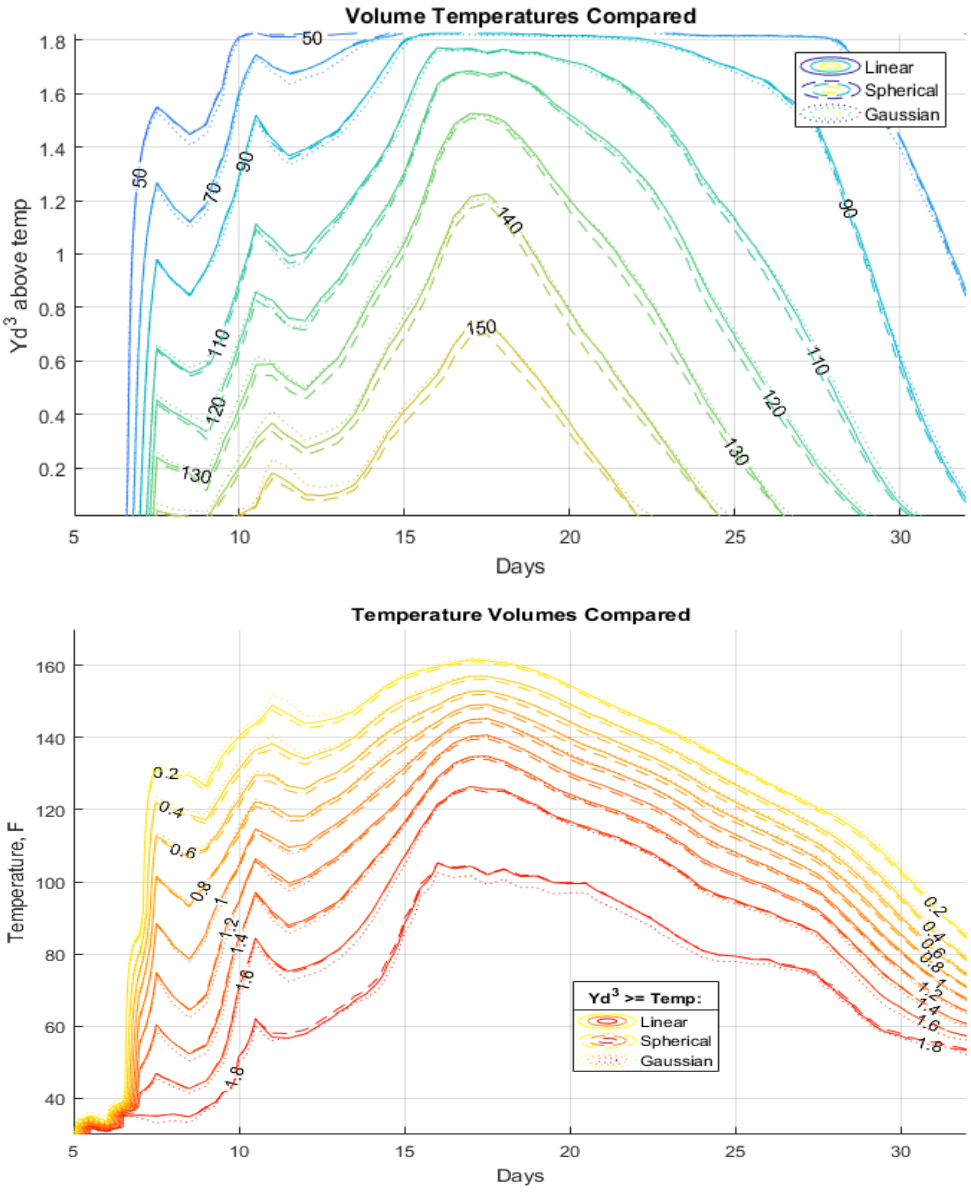

Figure 29: Volume Temperatures and Temperature Volumes Compared

Figure 30 (following page) compares the “specific” heat losses per model, in terms of accumulated heat loss (Megajoules) and power (W). The different colored contours correspond with the temperature above which the compost is considered “active”. While this is a rather arbitrary simplification, it is progressing towards the goal of determining the compost’s specific power. As seen, the difference in models increases at higher temperatures, while at 100 °F they are similar. At the higher “active” temperature, the spherical model shows greater specific power while the Gaussian shows less. This is because the volume of compost at or above 140 °F is smaller in the spherical model, and larger in the Gaussian model.

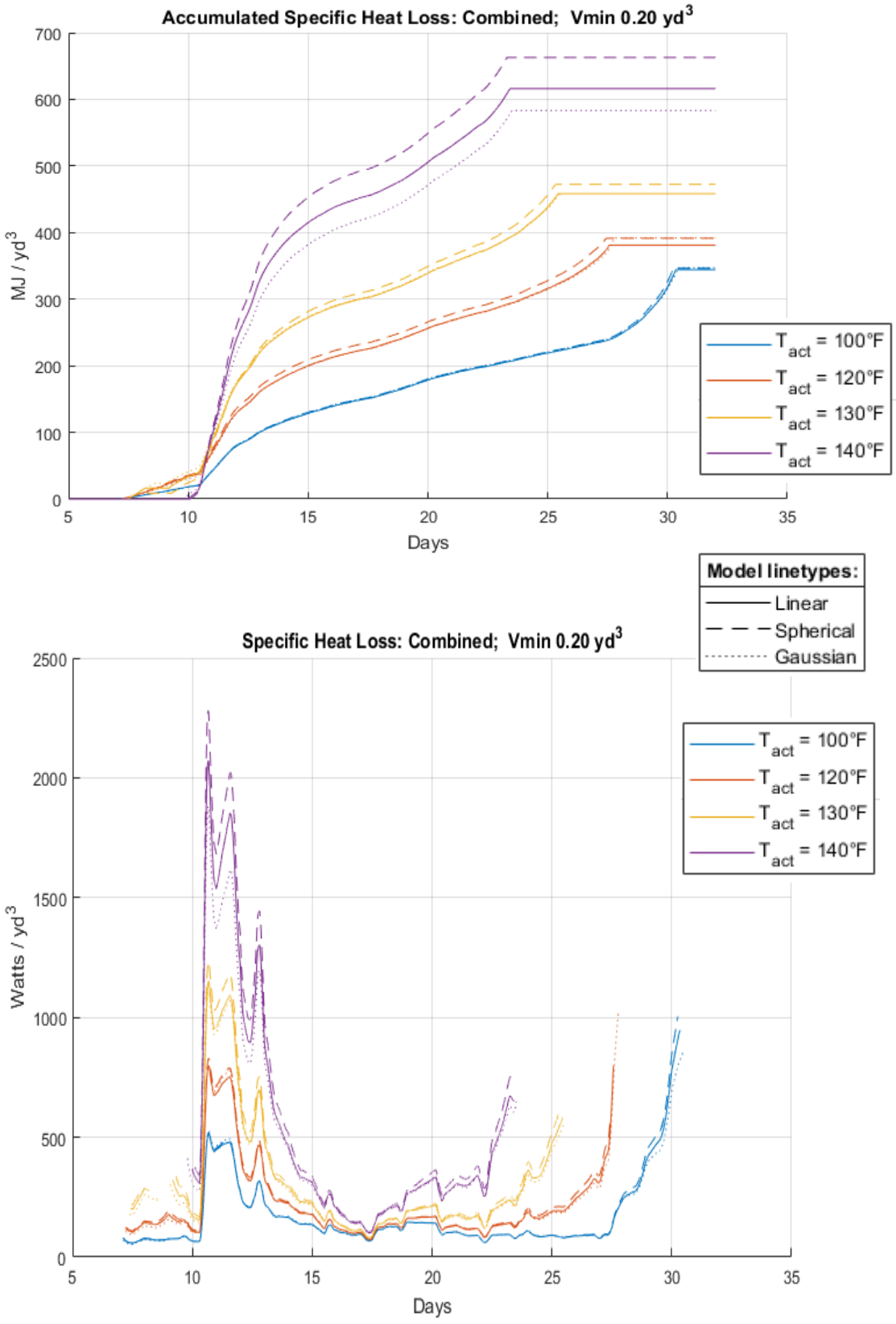

Figure 30: Specific Heat Losses Compared

6.3 Three-Dimensional Imagery

The best tool to qualitatively examine the temperature fields was found to be movies of the compost temperature isosurfaces, combined with volume temperature plots. Figures 31 and 32 show snapshots of these movies; selected files are attached to the thesis electronically. Figure 31 shows the modeled half domain corresponding with the results discussed so far. Figure 32 shows the same models over the full domain. Inspection of the 3-D images shows the comparative irregularity of the Gaussian model, which is visually interesting but seems less accurate. The Y > 22 half of the domain (that is included in the full domain plots) has less sensors, and none on the Y = 44 end which was the front door of the compost box. Here in particular the differences are apparent: the linear and spherical models display reasonable symmetry, while the Gaussian model extends the 160° isosurface to the edge, which is unlikely to have happened.

In comparing the full and half domain models, most outputs appear similar except the specific power figure, which is the most sensitive to differenced in volume temperature, does show a difference. At 140° active temperature, the specific power of the half domain tops out at around 2250 W (figure 28), while the maximum by the full domain (plot not shown) is around 1800 W.

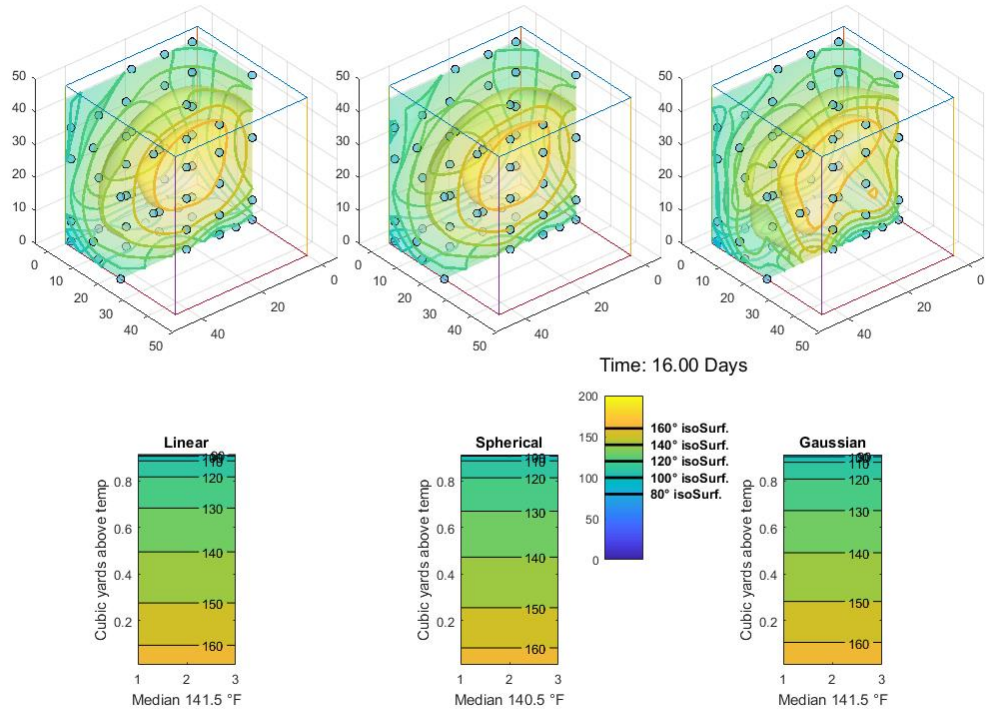

Figure 31: Half Box Heat Maps

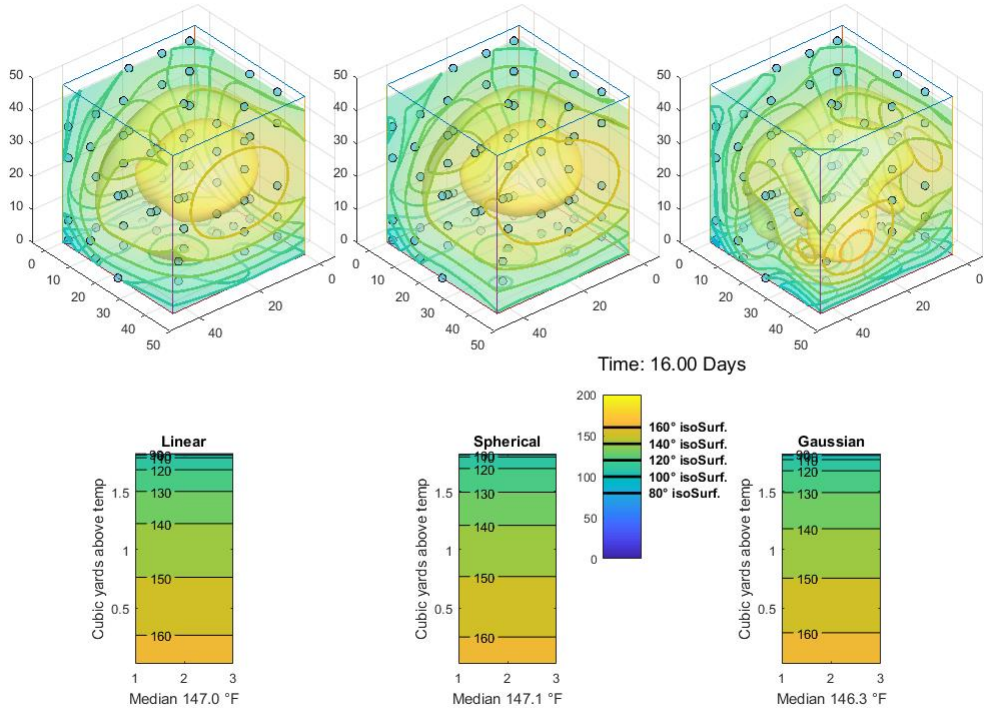

Figure 32: Full Box Heat Maps

Chapter 6: Conclusions and Future Work

The compost test vessel was successfully built using readily available materials. The design is simple and the most difficult part to obtain is the blower, which was ordered online. The scale and insulation were found to be sufficiently large and insulated to achieve thermophilic temperatures in cool ambient conditions. Heat loss from aeration was more difficult to control however, and a recirculation manifold is highly recommended for any future replications, or the ability to throttle airflow. 2" foam insulation panels proved rigid enough to hold the unit together without framing if they are fastened together somehow. The most difficult part of building the vessel was armoring the sides and corners from rodents, with 1/16" LDPE sheet and aluminum corner trim.

The control and monitoring system was more expensive and difficult to build, but with standardization and reduced sensor count it would be easier. Much of the cost and labor was in the large number of temperature sensors used; the controller and air flow meter were relatively cheap. Once constructed the system required little to no tending as it could be monitored and controlled remotely, and the control and data package is robust and can be re-used many time or repurposed. A better solution for plugging in the many 1-wire sensors is a continual mission. It would also be beneficial to find a device to capture WEL data on the local network.

Temperature fields were successfully modeled using Kriging techniques, and processed into forms than can be interpreted both quantitively and qualitatively. Initial assumptions of symmetry were found to be questionable, and thus smaller portions of the

domains with greater sensor density were analyzed. The conduction results from the selected geostatistical models were rather similar, especially since convection was a primary driver of heat loss. The temperature volumes were more variable.

Visualizing the temperature volumes is best done with movies of the temperature isosurfaces. These are valuable to assess the temperature patterns and plausibility of the model used. Another more surprising asset is the ability to see the compost temperatures moving with the aeration cycles, and observe the irregularities in this heat transfer. A known issue of aeration in vessels is preferential air flow along the walls, especially as compost shrinks and tends to slump away from the walls over time. Being able to observe the heat movement can help design the placement of aeration manifolds, which are biased towards the center to achieve more even aeration. Due to size limitations, these movies are not attached to the thesis, but may be available up on request or posted to YouTube in the future.

The compost temperature is of interest to estimate how much of the compost is active, and thus calculate the specific heat output. Future experiments, however, would be built with recirculation capabilities that would mix the compost temperatures, and allow for better control. With a more even compost temperature, the spatial models would be less sensitive, and most, or all, of the vessel could be considered heat producing. However it is still important to be able to visualize the compost temperature to see if portions are too cold or hot.

Geostatistical modeling can utilize irregular sensor arrays, which is generally an advantage. In this application the symmetry causes issues when there is an irregular density of sensors on opposite sides of the vessel. This could be addressed by further developing weighting / distancing techniques, or by using irregular sensors to build the semivariograms and find covariance models, then removing them from the Kriging program. More conventional interpolation or smoothing software might produce similar results with less effort. In any case, bounding the temperature field would be an advantage for a Kriging model, and a necessity for an interpolation model. Regardless of method, a future goal is to find the minimum sensor density that produces satisfactory results. It is expected that with a more even compost temperature, less sensors would be needed.

In terms of quantifying heat output and power of the compost, the most valuable results were 2-dimensional charts with contour of compost temperature volumes. Figure 33 shows the minimum temperature of compost volume bins, with heat losses by convection and conduction overlaid. The specific thermal activity of the compost is complex and difficult to model, as it relates to temperature, compost age, feedstock, moisture content etc. As age and temperature are major factors, this is helpful to estimate the specific heat output based on a judgement of compost activity.

For example, when the compost was hottest around 17 days, the heat loss hovered around 200 W, while almost all the volume was above 120 °F, in the active range. If we consider the entire volume of 1.8 cubic yards to be active, that would mean a specific heat output of around 110 W, or 378 Btu/h per yd^3. The greatest heat loss occurred just after initial warming of the compost around day 11. In that period, one might estimate that .6

cubic yards of compost were thermophilic, while releasing about 500 Watts through net enthalpy loss. However, it is evident that this rate of extraction cooled the compost significantly. Later, the system was basically stalling with minimal aeration. In a practical compost system, the material would have been turned at this point and would be expected to heat back up again before cooling into the curing phase. In Agrilab Technologies systems, the heat producing phase generally varies from 3 weeks to 2 months, with 1 to 6 turns, depending on the material and how it is handled; after that it is allowed to cure without aeration.

These heat production results need to be considered in context, as they represent the absolute heat released by the compost. Only a portion of this energy could be utilized

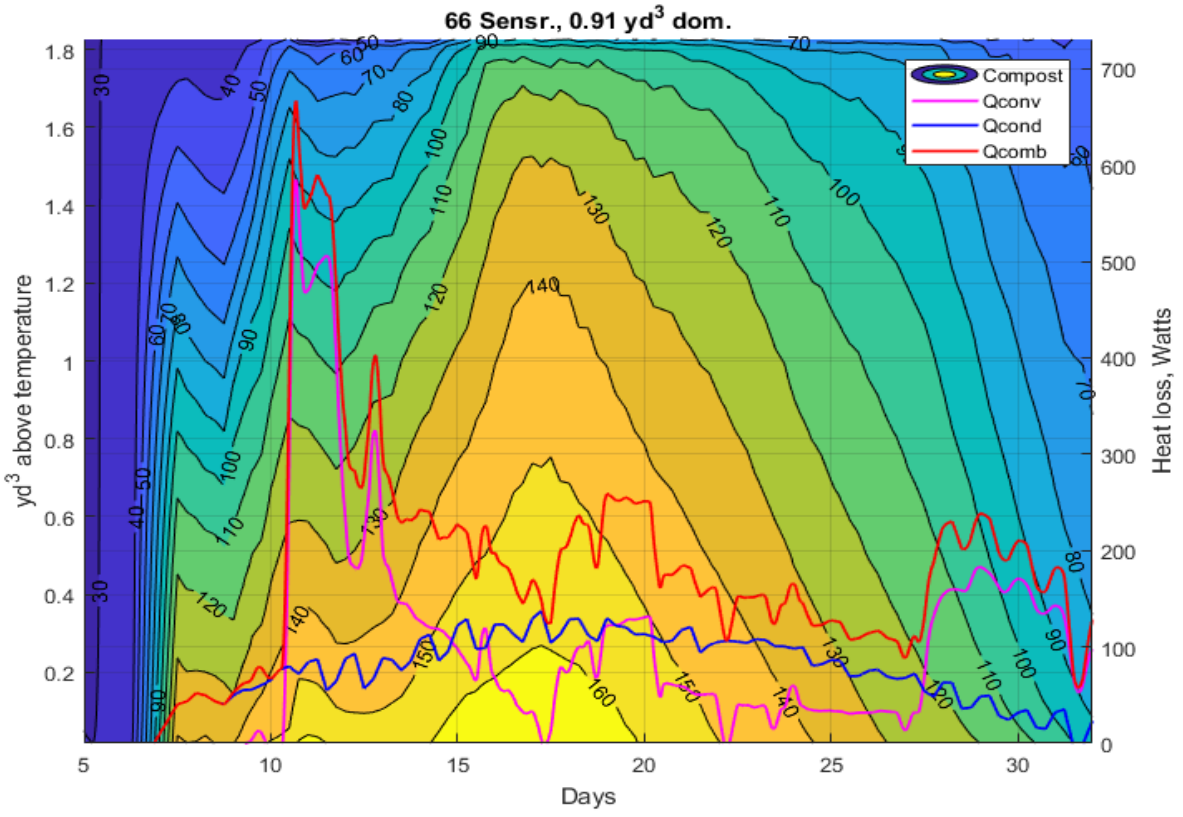

Figure 33: Compost Volume Temperatures with Heat Loss Overlaid

by a heating system, depending on the exhaust and use temperatures. In this experiment, the exhaust temperature only rarely approached temperatures that could be used by conventional heating systems, so a useful heat analysis was not included. With recirculation, the compost air can be mixed and then drawn, which should achieve useful exhaust temperatures. As saturated enthalpy accelerates with temperature, increased aeration temperatures are correspondingly more powerful and, assuming sufficient insulation, push the energy loss of the system towards convection; in effect, a greater portion of the compost heat would be useful.

These results are not considered to be a conclusive estimate of compost heat production, but the designs and analysis tools developed represent notable progress in the field, which remains largely unexplored in this manner. The test platform is robust and has already been prepared for another round of experimentation with an automated recirculation manifold. The Kriging models can be further examined to optimize sensor placement, and the ability to visualize the compost temperature in real time would be an operational asset. Once the platform is optimized, it should be inexpensive to test various feedstocks, and the system could be developed into a kit if there is demand. Comparing small vessel results to the temperature fields and heat yields of full scale CHR systems is ultimately of interest. Future test results can also help estimate the required sizes of small scale engineered compost heat systems for heat loads such as greenhouse heating or radiant shop floors.

References Cited

[1] R. T. Haug, The Practical Handbook of Compost Engineering, Ann Arbor: Lewis Publishers, 1993.

[2] R. Rynk, On-Farm Composting Handbook, Ithaca: National Resource, Agriculture and Extension Service, 1992.

[3] N. Themalis, "Control of Heat Generation during Composting," *Biocycle Magazine*, pp. 28 - 30, January 2005.

[4] Wikipedia Contributors, "Megapode," 24 June 2017. [Online]. Available: https://en.wikipedia.org/w/index.php?title=Megapode&oldid=787218086. [Accessed 7 November 2017].

[5] G. Brown, The compost-powered water heater, Woodstock: The Countryman Press, 2014.

[6] P. Aquatias, Intensive cultivation of vegetables on the French system, London: Upcott Gill, 1913.

[7] A. Loughton, "Straw-bale culture of greenhouse crops," in *Controlled environment agriculture*, Tuscon, University of Arizona, 1977, pp. 208 - 215.

[8] R. Queras, "Jean Pain The Power of Compost Part 1 (English Subtitles)," youtube, 28 January 2014. [Online]. Available: https://www.youtube.com/watch?v=XfmvbWrhfxQ. [Accessed 7 November 2017].

[9] I. Pain and J. Pain, Another kind of garden, Available as PDF, 1981.

[10] B. Fulford, "Biothermal Energy: Cogenerants of thermophylic composting and thier integratoin within food producing and waste recycling systems," in *Composting of solid wastes and slurries*, England, University of Leeds, 1983, pp. 1-19.

[11] M. Smith, J. Aber and R. Rynk, "Heat recovery from composting: a comprehensive review of system design, recovery rate, and utilization," *Compost Science & Utilization,* 2016.

[12] R. R. P. Jindal, "Modeling of Heat Generatoin in an Aerobic Composting Process," in *The 2nd Joint International Conference on Sustainable Energy and the Environment*, Bankok, 2006.

[13] D. C. M. T. W. K. S. Barrington, "Compost convective airflow under passive aeration," *Bioresource Technology,* vol. 86, pp. 259-266, 2003.

[14] F. C. Ferraro, B. Lohrer and M. M. M. Noll, "A mathematical model to predict the heating-up of large-scale wood piles," *Journal of Loss Prevention in the Process Industries,* vol. 22, pp. 439-448, 2009.

[15] T. S. H. N. M. Luangwilai, "Biological Self-Heating in Comost Piles: A Semenov Formulatoin," *Chemical Engineering Science,* vol. 101, pp. 533-542, 2012.

[16] C. M. N. R. M. Zambra, "Unsteady 3D heat and mass transfer diffusion coupled with turbulent forced convetion for compost piles with chemical and biological reactions," *International Journal of Heat and Mass Transfer,* vol. 55, pp. 6695-6704, 2012.

[17] B. E. C. X. Nelson. M.I., "A Semenov model of self-heating in compost piles," *Trans IChemE*, vol. 52, pp. 5841-5848, 2003.

[18] T. G. Poulsen, "Temperature, Pressure and Air Flow Distribution in Passively Aerated Compost Piles," *Compost Science & Utilization*, vol. 18, no. 2, pp. 127-134, 2010.

[19] P. Malone, "Web Energy Logger / intro," [Online]. Available: http://welserver.com/intro.htm. [Accessed 18 11 2017].